

LIBRARY  
ROYAL AIRCRAFT ESTABLISHMENT  
BEDFORD.

C.P. No. 1194



PROCUREMENT EXECUTIVE, MINISTRY OF DEFENCE

AERONAUTICAL RESEARCH COUNCIL

CURRENT PAPERS

A Review of some Published  
Data on the External-Flow  
Jet-Augmented Flap

by

*D. H. Perry*

*(with an Appendix by D. N. Foster)*

*Aerodynamics Dept., R.A.E., Farnborough*

LONDON: HER MAJESTY'S STATIONERY OFFICE

C.P. No. 1194



UDC 533.694.6 : 533.6.071

\*C.P. No. 1194  
December 1970

A REVIEW OF SOME PUBLISHED DATA ON THE EXTERNAL-FLOW  
JET-AUGMENTED FLAP

by

D. H. Perry

(with an Appendix by D. N. Foster)

SUMMARY

The data given in thirteen NASA papers describing wind-tunnel tests on external-flow jet-augmented flaps are reviewed. Details are given of the configurations tested and the main results achieved. Some of the data is compared with theoretical work done in the UK in support of internally ducted jet-flap schemes.

The application of jet-flap theory to the correlation of maximum lift coefficients, based on considerations of leading-edge loading, is given in an Appendix.

---

\* Replaces RAE Technical Report 70240 - ARC 32714.

CONTENTS

	<u>Page</u>
1 INTRODUCTION	3
2 PUBLISHED NASA WORK ON EXTERNAL JET FLAPS	4
3 AERODYNAMIC CHARACTERISTICS OF EXTERNAL-FLOW JET FLAPS	7
3.1 Static turning efficiency	7
3.2 Lift increments	9
3.3 Maximum lift coefficients	12
3.4 Longitudinal forces	12
3.5 Longitudinal stability and trim	14
4 DISCUSSION AND CONCLUSIONS	16
Appendix A Increase of the maximum lift coefficient of a wing section due to a jet-augmented flap - by D. N. Foster	19
Table 1	26
Symbols	27
References	30
Illustrations	Figures 1-23
Detachable abstract cards	-

## 1 INTRODUCTION

The jet-flap scheme<sup>1</sup> for integrating the lifting and propulsive systems of aircraft has been the subject of research for over two decades, culminating in the development of a research aircraft, the HS 126<sup>2</sup>. In Britain, most attention has been directed towards internally ducted schemes, where the engine efflux is conveyed through the wings and ejected from slots close to the trailing edge. Such schemes probably promise the greatest aerodynamic efficiency, but their practical application presents severe engineering problems in such matters as duct design, insulation, and utilization of space within the wing.

In the US some attention has been given to a simpler scheme in which the efflux from suitably positioned jet engines is directed externally over trailing-edge flaps of more-or-less conventional design (Fig.1). This arrangement has come to be known as the 'external-flow jet-augmented flap'. In many ways it emulates the slipstream effect which has been a familiar feature of propeller-driven aircraft.

The external jet flap obviously eliminates the need for complicated internal ducting, but not without introducing some problems of its own. It seems likely that means of spreading and directing the engine efflux towards the flaps will be required for reasonable lifting efficiency and thrust recovery. Problems may also arise in trimming the aircraft after an asymmetric engine failure, since there is generally no provision for redistributing the remaining jet efflux evenly across the wing.

The only detailed data on the external jet flap which has so far been published is that from work at the NASA research centres at Langley and Ames. It is believed that independent studies have also been made by some US airframe manufacturers, but data from these are not generally available.

The purpose of the present Report is to review the dozen or so NASA reports on this topic which have been issued since Campbell and Johnson published their first paper<sup>3</sup> in 1956. The general content of these papers is described in the following section 2, and certain aspects are then considered in more detail in section 3. The opportunity has also been taken to compare some of this data with theoretical work done in the UK in support of internally ducted jet-flap schemes.

2 PUBLISHED NASA WORK ON EXTERNAL JET FLAPS

NASA work on external-flow jet flaps has been reported in thirteen papers<sup>3-15</sup>, the majority from the Langley Research Centre. The main features of each study are listed in Table 1, and the more important configurations tested are illustrated in Figs.2-14.

Results of the first exploratory wind-tunnel tests were published by Campbell and Johnson<sup>3</sup> in 1956 (Langley Full Scale Tunnel). Preliminary experiments were made with an unswept rectangular wing of aspect ratio 6. Compressed air nozzles attached to the lower surface of the wing were used to represent the engine efflux, and the tests were made with both plain and slotted flaps. The results achieved were sufficiently encouraging to warrant further studies on a complete aircraft configuration, and these were made on a model of a typical transport aircraft, having a 30° swept wing and full-span slotted flaps (Figs.2 and 3). The primary emphasis in this investigation was on the lift, stability and trim aspects of the external jet flap. Tests were made with high-wing and low-wing layouts, with different numbers of engine pods, and with various tailplane sizes and positions. These studies indicated that lift coefficients of about 6 might be achieved, with reasonable values of installed thrust and tail plane size, but that stability and trim were likely to present difficult problem areas in the design of a jet-flap aircraft. In a subsequent paper<sup>4</sup> Johnson presented further data and analysis of these particular aspects.

Exploratory tests on a rectangular wing with double-slotted flaps were also reported by Davenport<sup>5</sup> (Langley 10ft × 7ft wind tunnel). The studies covered two different flap configurations and a variety of underwing nozzle arrangements, and the results presented include measurements of static turning efficiency, lift, drag and pitching moment.

Johnson extended the previous studies of trim and stability with tests of a free-flying model in the Langley Full Scale Tunnel<sup>6</sup>. The configuration tested was very similar to that used earlier (Figs.4 and 5). At the higher lift coefficients ( $C_L > 6$ ) it was not possible to achieve both trim and stability by conventional means. Stability could, of course, be achieved by moving the centre of gravity sufficiently far forward, but it was then necessary to resort to a downward pointing control jet in the nose for trimming.

The same model (Fig.4) was also used for further static wind-tunnel tests<sup>7</sup>, aimed at improving the efficiency of the external-flow jet flap. The methods investigated included the use of double-slotted flaps, in place of single-slotted flaps; the fitting of fish-tail nozzles to spread and deflect the engine efflux; modification of the wing undersurface profile, and the use of several nozzles spread out across the wing to increase the spanwise area affected by the jet momentum (Fig.5). These modifications brought about some improvement in static turning efficiency, and probably therefore in thrust recovery, but caused virtually no change in the component of lift attributed to supercirculation.

Meanwhile Turner, Riebe and Davenport (Langley 10ft x 7ft wind tunnel) were investigating configurations which used the efflux from engines mounted above the wing, pointing out, with some foresight in 1958, the possible advantages in noise suppression and debris ingestion with this arrangement. Preliminary tests<sup>8</sup> were made on an existing delta wing model of aspect ratio 3 (Fig.6). Although significant lift increments were achieved, the problems of trimming such a configuration are particularly severe. Further studies<sup>9</sup> of the overwing arrangement were made on a 35° swept wing of aspect ratio 7 (Fig.7). Various types of flap and nozzle were tested, and the results presented included the usual measurements of static turning efficiency, lift, drag and pitching moment. The best combination of flap and nozzle gave a static turning efficiency of 0.9 at a deflection angle of 60°, a value rather higher than any other reported in the papers reviewed. Several novel methods of achieving stability and trim were investigated. They included a canard fore plane, and tails mounted on booms attached to the outer wings, in an attempt to find a position for the stabilizer away from the adverse downwash field immediately behind the flaps.

The last of these early investigations was made by Fink<sup>10</sup> (Langley Full Scale Tunnel) on a large model of some 32 ft span (Fig.8). While all the earlier tests had used compressed air to simulate the engine efflux, this model was fitted with two small turbojet engines, each producing a thrust of about 1000 lb. They were mounted on underwing pylons and fitted with fish-tail nozzles to provide a flattened jet sheet directed upwards towards the flaps. Single-slotted flaps, extending over either half or the whole of the span, were tested. The aerodynamic measurements made on this large model broadly confirmed the data gathered in earlier investigations. In addition, measurements were made of skin temperatures and sonic pressure fluctuations in those regions where the jet impinged upon the wing.

Following these tests, an interval of some six years elapsed before the publication of any further work by NASA on the external-flow jet flap. From an aerodynamic and performance viewpoint the characteristics revealed by the early tests had been quite attractive, but it is believed that a number of other factors made the immediate adoption of the external-flow scheme impractical. Chief amongst these were:

(1) Structural problems in designing the wing and flap to withstand the high exhaust temperatures of the jet engines then in use.

(2) High noise levels associated with running such engines at their maximum rating.

(3) The lack of a suitable framework of airworthiness requirements for certificating 'powered-lift' aircraft for civil operation.

The advent of engines with much higher by-pass ratios has gone some way towards easing the first two of these problems, while the third is being more actively tackled as a result of current interest in VTOL and STOL aircraft. The removal of these constraints probably accounts for the recent revival of work on external-flow schemes. Coupled with this must be the possibility of achieving direct-lift control (DLC) of the flight path by means of a small auxiliary flap attached to the rear of the main flap.

The first of the more recent tests was directed primarily towards this latter aspect. In 1967 Kirk, Hickey and Aoyagi (Ames 40ft x 80ft wind tunnel) reported<sup>11</sup> tests on a large scale model of generally similar layout and dimensions to that used earlier by Fink (Fig.9). The results presented show that adequate long term control of flight path by means of an auxiliary flap could be achieved. However, the direct effect of the auxiliary flap on lift was small, particularly at the larger flap angles, so that the benefits of faster response to lift demands, normally sought in a DLC system, were not achieved. These studies were continued by Aoyagi, Dickinson and Soderman<sup>12</sup> on another large scale model of a four engined transport aircraft (Fig.10), as part of a combined wind-tunnel and flight test<sup>26</sup> investigation into DLC. In this case flow attachment over the main flaps was ensured by blowing boundary layer control, using air tapped from the engine compressors. The tests showed that acceleration increments of  $\pm 0.2$  g should be obtainable by deflecting the auxiliary flaps, at a typical landing condition, and it is believed this provides a reasonable margin for manoeuvring.



The first tests in which engines of high by-pass ratio were used in conjunction with external-flow flaps were reported by Parlett, Fink and Freeman<sup>13</sup> (Langley Full Scale Tunnel). A novel feature of this study was the use of miniature fan jet engines, driven by compressed nitrogen, to simulate the engine efflux. The model represented a current long-range transport aircraft, but the pylons of the underwing mounted engines had been shortened to give more direct impingement of the engine efflux onto the flaps (Figs.11 and 12). There was no provision for deflecting the engine efflux towards the flaps, nor were the flaps designed for this jet-flap application. In consequence, measurements of turning efficiency and lift increments showed a relatively poor performance, compared with that achieved in the earlier studies. Dynamic stability measurements, using an oscillatory rig, have also been reported<sup>14</sup> by Freeman, Grafton and Amato for this configuration. These tests revealed no unexpected characteristics.

Finally, Parlett and Shivers (Langley Full Scale Tunnel) have described<sup>15</sup> tests on a transport aircraft model with an unswept wing of aspect ratio 7 (Figs.13 and 14). This configuration was chosen with a view to possible STOL applications of the external jet-flap principle. The engine efflux from high by-pass ratio engines was simulated by ejector nozzles, using compressed nitrogen. A feature of these tests was a marked longitudinal instability which occurred at quite modest angles of incidence. This was attributed to the wing-tip vortices being drawn into the region of the tail by the high concentration of lift over the inboard areas of the wing. Efforts which were made to produce a more even spanwise distribution of lift resulted, however, in negligible improvements in stability.

### 3 AERODYNAMIC CHARACTERISTICS OF EXTERNAL-FLOW JET FLAPS

#### 3.1 Static turning efficiency

The static turning efficiency is usually taken to be the ratio of the resultant forces with the flaps deflected, and with the flaps retracted, both being measured under static conditions. It may therefore be regarded as a measure of the impingement and turning losses involved in using the flaps simply as thrust deflectors. Most of the papers discussed previously give some data on this topic. The measured longitudinal and normal components of the redirected thrust may be presented conveniently on a polar plot, such as that shown in Fig.15, from which the turning efficiency and effective jet deflection angle can be obtained directly.

The early work of Campbell and Johnson<sup>3,4,6</sup> showed that turning efficiencies of about 0.8 could be achieved for flap deflections of  $40^{\circ}$ - $50^{\circ}$ , reducing to about 0.7 at a flap angle of  $70^{\circ}$ . These results were obtained on underwing installations, with a simple flat-plate deflector to direct the engine efflux upwards towards a suitably designed slot in the flaps (Fig.3). Similar results have also been obtained recently by Parlett and Shivers<sup>15</sup> in tests simulating the flow from a high by-pass ratio engine (Fig.14). In attempting to improve upon these values of turning efficiency Johnson<sup>7</sup>, and later Fink<sup>10</sup>, fitted fish-tail shaped nozzles to spread and deflect the jet sheet towards the flaps (Figs.5 and 8). Turning efficiencies with this arrangement were improved by about 10 per cent over those with the simple flat-plate deflector, but it may be noted that Johnson's tests<sup>7</sup> showed no accompanying increase in the lift due to supercirculation.

The need for considerable care in the design of the flaps, nozzles and deflectors is well illustrated by the data given by Parlett<sup>13</sup> for a configuration which was not designed specifically for jet-flap application (Fig.12). In discussing the low turning efficiencies measured in these tests (see Fig.15) the authors comment: "A probable cause for these low static efficiencies is that the flap system was not designed specifically for a jet-flap application. The jet exhaust impinged directly on the main flap and caused most of the turning to take place below the flap system; the data from a previous study indicate that better turning would have resulted if the jet exhaust had been spread out, flattened and directed towards the flap gaps, so that the turning would have been more gradual and more of the turning could have been done by the upper surfaces of the flap system."

The results described above for underwing installations are summarized in Fig.15. Two curves are tentatively suggested for project studies when more specific data is lacking. Both relate to suitably designed flaps, but in one case the jet exhaust is spread by a fish-tail shaped nozzle, while in the other the simpler, but less efficient, flat-plate deflector is assumed.

The small amount of data for overwing installations<sup>8,9</sup> suggests that such arrangements may be even more sensitive to the detail design of flaps and deflectors than their underwing counterparts. Tests<sup>8</sup> on a delta wing of aspect ratio 3 (Fig.6) gave values of static turning efficiency not exceeding 0.5-0.6, even for small deflection angles. On the other hand, the best configuration studied in the other overwing tests<sup>9</sup> (Fig.7) yielded turning efficiencies of 0.9 at deflections of  $60^{\circ}$ ; a better result than that achieved on any of the underwing installations.

The variation of turning efficiency with thrust level has not been extensively investigated. Tests by Davenport<sup>5</sup> on a straight wing with underwing blowing showed no significant variation, but both the studies of overwing blowing mentioned above<sup>8,9</sup> showed some variation, although not in a consistent manner.

It is of interest to compare the results discussed above with the turning efficiency of deflecting devices fitted directly to the engine. Ashwood<sup>16</sup> quotes thrust losses of 10½ per cent for deflectors designed to give a 60° turning angle, which were fitted to a research aircraft. Of this loss 2½ per cent was attributed to leakage along the main jet pipe. (The installation caused thrust losses of about 5 per cent in normal forward thrust, of which about one half was believed to be due to leakage.) Wilde<sup>17</sup> also quotes losses of from 5-8 per cent in gross thrust for deflectors of both the rotating cascade and simple two position types.

### 3.2 Lift increments

Extensive theoretical and experimental work on both blown and jet flaps has established<sup>1</sup> the jet momentum coefficient  $C_{\mu} \left[ = \frac{M_J V_J}{q_0 S} \right]$  as the major non-dimensional parameter for the correlation of results. In the case of the external-flow jet flap the whole of the engine efflux is involved so that, neglecting losses, the jet momentum is equal to the gross thrust of the engines.

Fig.16 illustrates the typical variation of lift coefficient with jet momentum coefficient for a given angle of incidence and flap deflection. In analysing such data it has been the practice at the NASA to consider the lift coefficient as comprising three components; a basic lift coefficient  $(C_L)_{C_{\mu}=0}$  at zero jet momentum; a direct jet reaction component, taken as either  $C_{\mu} \sin(\delta_J + \alpha)$  or  $\eta C_{\mu} \sin(\delta_J + \alpha)$ ; and a remaining component  $C_{L_F}$  representing the circulation lift induced by the jet sheet. The latter is sometimes termed the 'lift due to supercirculation'. All three of these components are illustrated in Fig.16.

It is often difficult to gauge the practical significance of the jet flap from data such as Fig.16. This is because the value of  $C_{\mu}$  for a given thrust depends (by its definition) on the aircraft's speed, but this is often governed, in turn, by what lift coefficient the wing can generate. A better

assessment of the potentiality of jet-flap schemes may possibly be gained from a plot of  $C_L$  against  $C_\mu/C_L$  (Fig.17), rather than against  $C_\mu$  alone. In '1 g' flight the parameter  $C_\mu/C_L$  is roughly equivalent to the thrust/weight ratio of the aircraft. Hence, the  $C_L$  vs  $C_\mu/C_L$  plot indicates what lift coefficients are available at different levels of installed thrust. There are, of course, other factors which must be considered as well, such as whether these lift coefficients can be obtained without excessive angles of climb or descent.

A theoretical treatment of the jet flap in twodimensional inviscid flow was first developed by Spence<sup>18,19</sup>, using thin-aerofoil theory. This treatment was later extended to the threedimensional case by Maskell and Spence<sup>20</sup> employing the classical methods of Lanchester and Prandtl. Using this theoretical framework, backed by a number of experimental results on internally-ducted jet flaps, Williams, Butler and Wood<sup>1</sup> have suggested the following relationship for the lift on a jet-flapped wing of finite aspect ratio, with full-span, or part-span flaps.

$$C_L = F \left[ \left( 1 + \frac{t}{c} \right) \left\{ \lambda \theta \left( \frac{\partial C_L}{\partial \theta} \right)_\infty + \nu \alpha \left( \frac{\partial C_L}{\partial \alpha} \right)_\infty \right\} \right] - \frac{t}{c} C_\mu (\theta + \alpha) \quad (1)$$

where  $\theta$  is the jet deflection angle,  $\alpha$  the incidence, and  $F$  a factor to account for finite aspect ratio, based on the theoretical work of Maskell and Spence<sup>20</sup>:

$$F = \frac{A + \left( \frac{2C_\mu}{\pi} \right)}{A + 2 + 0.604 C_\mu^{1/2} + 0.876 C_\mu} \quad (2)$$

$\lambda$  and  $\nu$  are allowances for part-span effects, being given by:

$$\lambda = S'/S \quad (3)$$

$$\nu = \frac{S' \left( \frac{\partial C_L}{\partial \alpha} \right)_\infty + (S - S') \left( \frac{\partial C_L}{\partial \alpha} \right)_{\infty, C_\mu=0}}{S \left( \frac{\partial C_L}{\partial \alpha} \right)_\infty} \quad (4)$$

$S$  is the total wing area, and  $S'$  the wing area affected by the jet flap.

Theoretical values of the derivatives  $\left(\frac{\partial C_L}{\partial \theta}\right)_{\infty}$  and  $\left(\frac{\partial C_L}{\partial \alpha}\right)_{\infty}$  as functions of flap chord and jet momentum coefficient have been given by Spence<sup>19</sup>.

Williams<sup>1</sup> has compared the lift coefficients predicted by equation (1) with experimental data for internally ducted jet flaps. The agreement was very good up to jet deflection angles of about  $40^\circ$ , but the experimental results at higher deflections were somewhat below those predicted, as might be expected with a theory based on linearised relationships.

Fig.18 shows the results of a similar comparison for some of the NASA experimental data on external-flow jet flaps. To take account of the fairly large turning and impingement losses revealed by the static calibrations (section 3.1), the jet momentum coefficients used in evaluating equation (1) were based on the gross engine thrust, factored by the measured static turning efficiency. For the twin-podded arrangements, where the jet efflux obviously did not cover the whole of the flap span, an estimate was made of the wing area thought to be affected by the supercirculation. Considering the obvious differences between the external flow arrangement and the idealised jet flap for which the theory was developed, the agreement shown in Fig.18 between theory and experiment is remarkably good. The measured lift coefficients are, on average, some 10 per cent below those predicted, while the scatter is of the same order.

A detailed examination of the comparison shown in Fig.18 revealed certain consistent trends in the discrepancies between measured and predicted data. Although these trends could not be explained, they enabled an even closer correlation to be achieved, as shown in Fig.19, by the introduction of two empirical correction factors, one depending on the jet deflection angle (Fig.20a) and the other on the jet momentum coefficient (Fig.20b). In the absence of other data it is suggested that preliminary estimates of the lift increments from external jet flaps can be obtained by applying these two factors  $f_1(\delta_J)$  and  $f_2\left(C'_{\mu_e}\right)$  from Fig.20 to values estimated from equation (1).

It should be observed that the test data used in the above comparison related primarily to those studies where special care was taken to spread the jet efflux, and where the flaps were suitably designed for this application. It is clear from some of the other studies referred to that much inferior results may be obtained if these precautions are not observed.

### 3.3 Maximum lift coefficients

The thin-aerofoil theory<sup>19</sup> used successfully by Spence to predict the lift increments due to a jet flap can give no direct guide as to the maximum lift coefficients achievable, since it deals essentially with inviscid flow. However, McRae<sup>21</sup> has suggested that a relationship between the maximum lift coefficients of a wing with and without trailing-edge flaps can be derived from a consideration of their sectional pressure loadings. This applies to aerofoils having a 'leading-edge' type of stall<sup>22</sup>, and is based on the hypothesis that flow separation will occur when the leading edge loading reaches a certain value for a given aerofoil. McRae deduces that the increments in  $C_{L_{max}}$  due to a trailing-edge flap, in twodimensional flow, should be roughly one half of the lift increment at constant incidence. For wings of finite aspect ratio the factor is modified to be  $\frac{1}{2} \left( \frac{A+2}{A} \right)$ .

In Appendix A of this Report, D. N. Foster has applied the same hypothesis to Spence's jet-flap theory, and concludes that an analogous relationship for a flap in twodimensional flow with supercirculation is:

$$\Delta C_{L_{max}} = \frac{1}{2} \left( \Delta C_{L_{\delta, C_{\mu}}} + \frac{1}{2} C_{L_{C_{\mu}}} \right) \quad (5)$$

where  $\Delta C_{L_{\delta, C_{\mu}}}$  is the lift increment at constant incidence due to deflection and jet augmentation, taken together, while  $\Delta C_{L_{C_{\mu}}}$  is the lift increment due to jet augmentation with the flap already deflected. These measurements should be evaluated at the stalling incidence, ignoring flow separation effects.

To test this analysis, Fig.21a shows values of  $\Delta C_{L_{max}}$  plotted against the term in brackets in equation (5), for the lift data from Ref.10. The experimental points are seen to be well disposed about a straight line having a gradient slightly below the theoretical<sup>†</sup>. The absence of data for the flaps up configuration in Ref.7 does not allow the increments for this study to be checked in the same way, but Fig.21b shows that  $C_{L_{max}}$  varies with  $C_L$  at  $\alpha = 0$  in the expected manner.

### 3.4 Longitudinal forces

The close integration of the lifting and propulsive systems inherent in a jet-flap arrangement makes it difficult to analyse the longitudinal forces in

<sup>†</sup> Strictly speaking the correction for aspect ratio and therefore the slope of these plots should be  $1/F$  instead of  $\frac{A+2}{A}$  but this would preclude the comparison of data from tests at different values of  $C_{\mu}$ . For the values of  $C_{\mu}$  used in these tests the discrepancy lies within the scatter.

the conventional way, i.e. in terms of separable thrust and drag components, modified by interference effects, but only in a second-order manner. For the jet flap such 'interference' effects are of primary importance, and the overall longitudinal force should therefore be considered as a single entity. This makes the interpretation of experimental data, in particular, extremely complex and difficult. Consequently, although longitudinal force measurements have been made in all the NASA studies, they have so far only been used in a rather *ad hoc* manner in project assessments. In practice the achievement of low 'drag' and good 'thrust recovery' are likely to prove crucial in attaining the required climb performance during take-off, particularly in the critical airworthiness condition with one engine failed. During landing, on the other hand, the main difficulty may lie in producing a longitudinal force compatible with a descending flight path, at the high jet momentum coefficients needed to generate the desired lift.

According to inviscid flow theory, the efflux from a jet flap in twodimensional flow would ultimately become parallel to the free stream, and the longitudinal force should therefore be equal, ideally, to the total jet momentum, whatever the initial deflection of the jet. This is sometimes referred to as the 'thrust recovery' hypothesis.

For wings of finite aspect ratio, Maskell and Spence derived<sup>20</sup> the following expression for the net longitudinal force coefficient (denoted here by  $C_A$ , in accordance with the scheme of nomenclature suggested by Hopkin<sup>23</sup>):

$$C_A = C_\mu - \frac{C_L^2}{\pi A + 2C_\mu} - C_{D0} \quad (6)$$

where  $C_{D0}$  accounts for the basic skin friction and form drag. Even the briefest examination of the experimental data shows that equation (6), as it stands, does not adequately predict the longitudinal forces for external flow jet flaps.

Williams<sup>1</sup> suggested the more general form:

$$C_A = rC_\mu - \frac{kC_L^2}{\pi A + 2C_\mu} - C_{D0} \quad (7)$$

where the factors  $r$  and  $k$  are introduced to allow for deficiencies in the recovery of jet momentum, and departures from the idealised spanwise loading assumed in deriving equation (6). But, as Williams pointed out, it is often

difficult, from a small amount of experimental data, to establish the necessary functional relationships for  $r$  and  $k$ . With the present data for external flow jet flaps, the obvious step of substituting the static measurement of turning efficiency  $\eta$  in place of  $r$  did not yield any obvious correlation for the remaining factor  $k$ .

Yet another relationship, used by Wood<sup>24</sup> in estimating the performance of the HS 126 research aircraft, mentioned earlier, is:

$$C_A = rC_\mu - C_{D_0} - \Delta C_{D_{Of}} - \frac{C_L^2}{\pi A + 2C_\mu} - k_1 (C_L - C_{L_0})^2 \quad (8)$$

where  $C_{D_0}$  and  $\Delta C_{D_{Of}}$  are the profile drag coefficients of the aircraft and flaps at zero jet momentum;  $k_1$  is an incremental drag factor, and  $C_{L_0}$  is the lift coefficient for minimum drag (taken to be a function of  $C_\mu$  and  $\delta$ ). Unfortunately the validity of this expression for the external jet-flap data could not be investigated because the available measurements did not cover a sufficiently wide range of negative incidence for  $C_{L_0}$  to be established.

In view of the apparently good correlation established between theoretical predictions and experimental data in the case of lift (section 3.2), it is perhaps regrettable to have to report that the most satisfactory correlation for the longitudinal forces was obtained by largely ignoring jet-flap theory. Treating the flap as a simple thrust deflector, but taking into account the lift due to supercirculation, the conventional analysis of longitudinal forces gives the expression:

$$C_A = \eta C_\mu \cos(\alpha + \delta_J) - \frac{\left[ (C_L)_{C_\mu=0} + \Delta C_{L_\Gamma} \right]^2}{\pi A} - C_{D_0} \quad (9)$$

In Fig. 22 experimental data from Ref. 10 is presented in the form of plots of  $C_A - \eta C_\mu \cos(\alpha + \delta_J)$  against  $\left[ (C_L)_{C_\mu=0} + \Delta C_{L_\Gamma} \right]^2$ . Data for various jet momentum coefficients and angles of incidence are seen to lie on three parallel straight lines, having the correct theoretical slope of  $1/\pi A$  and distinguished only by the three different flap angles tested.

### 3.5 Longitudinal stability and trim

Longitudinal stability and trim was recognized from the outset as a potential problem area with external-flow jet flaps (as indeed with the internal-flow type) and it has consequently received considerable attention. Two main



difficulties arise. Firstly, the generation of a large proportion of the lift towards the rear of the aerofoil leads to severe nose-down pitching moments, and the consequent need for a very powerful tail plane to maintain longitudinal trim. Secondly, experiments have shown that the downwash derivative  $\frac{\partial \epsilon}{\partial \alpha}$  approaches the critical value of unity, at which the tail plane becomes destabilizing, for many normal tail plane locations.

Johnson<sup>4</sup> compared the merits of various trimming devices, with the position of the centre of gravity adjusted to give a constant static margin of 0.1 c. They included conventional tails of various sizes; fixed and freely floating (i.e.  $\frac{\partial C_{L_T}}{\partial \alpha} = 0$ ) canard surfaces, and trimming jets at the nose or tail. For conventional tails, increasing the area allows the centre of gravity to be moved back closer to the centre of pressure of the flaps, thus alleviating the trimming problem. In the early studies<sup>3,4,6</sup> a CG position of 0.40 c, combined with a tail plane area of about 25 per cent of the wing area, was found to give adequate trim and stability up to lift coefficients of about 6. However, some difficulty would probably be experienced in accommodating as wide a range of CG position as is available on current transport aircraft (i.e. typically 0.20 c).

Johnson's study<sup>4</sup> indicated that a fixed canard arrangement, with jet augmentation, would provide trim and stability at a given lift coefficient for less overall jet momentum than the other methods investigated. A similar arrangement was also studied by Turner *et al.*<sup>9</sup> Although this gave a satisfactory trimming moment, it was found that up to one half of the canard lift was effectively lost due to interference effects on the wing lift.

Fig.23 shows the variation in downwash factor  $\left(1 - \frac{\partial \epsilon}{\partial \alpha}\right)$  with jet momentum coefficient for two positions of a conventional tail plane studied in Ref.4. The large reduction in downwash factor with increasing  $C_{\mu}$  is similar to that measured in some internal-flow jet-flap tests<sup>1</sup>. It conflicts with theoretical predictions<sup>25</sup>, but this is probably because the present theory neglects the effects of rolling up the trailing vortex sheets. Flow visualization studies by Parlett<sup>15</sup> have shown such effects to be very severe, particularly when the spanwise lift loading is concentrated over the central portions of the span. Despite the mounting of the tail plane in an apparently favourable position (Fig.13) the data given in Ref.15 show that instability develops at quite modest angles of incidence. Close to the stall the effect of the tail plane was destabilizing, indicating that the downwash factor  $1 - \frac{\partial \epsilon}{\partial \alpha}$  was negative.

4 DISCUSSION AND CONCLUSIONS

The experimental studies reviewed in this Report have clearly established that lift coefficients substantially in excess of those obtained with mechanical flaps can be generated using the external-flow jet-flap principle. These lift coefficients are also appreciably greater than would be obtained by simply deflecting the jet thrust.

Theoretical methods for predicting the lift increments of internal-flow jet flaps appear to hold quite well for efficient external-flow flaps as well, when account is taken of the reduction in effective jet momentum due to turning and impingement losses. However, it is evident that care must be taken in spreading and deflecting the jet momentum, so that it approximates to the thin jet sheet assumed in jet-flap theory, if good results are to be obtained. Some problems may be foreseen in achieving this with the larger air mass flows associated with engines of high by-pass ratio.

An application of jet-flap theory by D. N. Foster (Appendix A) gives a method of correlating the maximum lift coefficients of jet-flap wings, on the basis of the pressure loading close to the leading edge of the aerofoil. The results of applying this method to wind-tunnel data on external-flow jet flaps were encouraging.

It can be shown theoretically that the whole of the jet momentum issuing from a jet flap should be recovered as thrust, and some measure of this 'thrust recovery' has been demonstrated during experimental work on internal-flow jet flaps. It is not evident, however, from the published data reviewed in this Report that the same effect can be relied upon with the larger amount of mixing between the jet and free stream which might be expected to occur in the external-flow scheme. In the absence of further data it seems safer to assume that only the resolved component of the jet momentum (corrected for turning and impingement losses) produces thrust in the longitudinal direction.

The published data shows that longitudinal trim and stability problems with the external-flow jet flap may be severe. As with any high-lift system which generates a large proportion of the lift over the rear of the aerofoil, large nose-down pitching moments are produced for CG locations which give adequate stability. To compound this problem, experimental studies have shown that the downwash derivative  $\frac{\partial \epsilon}{\partial \alpha}$  approaches the critical value of unity at high jet momentum coefficients for many normal tail plane positions. This effect is analogous to the destabilizing effect of propeller slipstream studied by Morris and Morrall<sup>27</sup>.

There are, of course, many other aspects of the external-flow jet-augmented flap which will need to be considered in any practical application. One of the more important of these, for civil operations, is that of far-field noise. Maglieri and Hubbard<sup>28</sup> made some preliminary measurements of jet noise on a number of possible jet-flap configurations, both of the internal-flow and external-flow types. Their test results indicated that the jet noise in the downward direction could be larger, by up to 10 dB, for an underwing jet-flap configuration (such as that shown in Fig.3) compared with that from a conventional underwing installation. With engines of the higher by-pass ratios now coming into use the importance of jet noise is somewhat diminished, and noise from the fan tends to be the critical factor. As far as is known there is no data yet published on the fan noise of external-flow jet-flap configurations, but from simple considerations of sound reflection it seems inevitable that some increase in downward fan noise will be produced.

•

,

## Appendix A

### INCREASE OF THE MAXIMUM LIFT COEFFICIENT OF A WING SECTION DUE TO A JET-AUGMENTED FLAP

by

D. N. Foster

In this analysis, an attempt will be made to evolve a simple relationship between the maximum lift coefficient of a plain wing section, and the maximum lift coefficient of the same wing section when fitted with a jet-augmented flap. The analysis will be limited to aerofoil shapes for which the plain wing section, and the section with a deflected flap, with or without jet-augmentation, all exhibit the same type of stall, a leading-edge stall. Under these circumstances, it might be expected that, at the stall, the pressure distribution around the leading edge for the flapped wing section would be similar to that for the plain wing section. To establish that pressure distributions around a given leading edge are similar, it is probably only necessary to show that the pressure difference between any two points on the upper and lower surfaces near the wing leading edge is unaltered by the deflection of the flap, and the use of jet augmentation. These two points may be assumed to lie on the upper and lower surface of the wing section at the same chordwise station. Such an assumption has, in fact, some similarity to the successful use by Multhopp<sup>29</sup> of the thickness of the wing leading-edge shape, at a given chordwise station, in the correlation of the maximum lift coefficient of plain aerofoil sections with varying thickness.

Weber<sup>30</sup> has shown that, for a thick aerofoil of symmetrical section, the pressure coefficient at any given point on the surface of the aerofoil is related to that on a thin aerofoil at the same angle of incidence by factors dependant on the thickness distribution of the wing section. For an aerofoil section of given thickness, these factors will not be altered by the deflection of the flap, and thus a qualitative assessment of the effect of flap deflection on the pressure distribution around the leading edge of a thick aerofoil may be obtained from a consideration of the pressure distribution for a thin aerofoil.

Initially, a datum value of the pressure difference, denoted by  $(-\Delta C_p)$ , must be established for the plain aerofoil. For the thin aerofoil at an angle of incidence  $\alpha$ , the lift coefficient  $C_L$  is given by

$$C_L = 2\pi\alpha \quad (A-1)$$

and the pressure difference by

$$(-\Delta C_p) = 4\alpha \sqrt{\frac{1-x}{x}} .$$

If the chordwise distance  $x$  is related to an angle  $\theta$  by

$$x = \frac{1}{2}(1 + \cos \theta) \quad (\text{A-2})$$

then the pressure loading  $(-\Delta C_p)$  can be written as

$$(-\Delta C_p) = 4\alpha \tan \frac{\theta}{2} . \quad (\text{A-3})$$

Near to the leading edge  $x \rightarrow 0$ , and  $\theta \rightarrow \pi$ .

Thus if  $\theta = \pi - 2\epsilon$ , and  $\epsilon$  is small,

$$(-\Delta C_p) = 4\alpha \frac{1}{\tan \epsilon}$$

which to order  $\epsilon^2$  is

$$(-\Delta C_p) = \frac{4\alpha}{\epsilon} .$$

Hence if the critical value for a leading-edge stall at a chordwise position corresponding to  $\epsilon_s$  is  $(-\Delta C_{p_s})$ , then

$$\left(-\Delta C_{p_s}\right) = 4 \frac{\alpha_s}{\epsilon_s} ,$$

or in terms of the lift coefficient

$$\left(-\Delta C_{p_s}\right) = 2 \frac{C_{L \max}}{\pi} \frac{1}{\epsilon_s} . \quad (\text{A-4})$$

Consider now a plain flap without blowing or jet augmentation, of chord ratio  $c_f/c$ , and deflection  $\delta$ .

Following Spence<sup>19</sup> the lift coefficient is then

$$C_L = 2\pi\alpha + 2(\chi + \sin \chi)\delta \quad (\text{A-5})$$

where

$$1 - c_f/c = \frac{1}{2}(1 + \cos \chi) \quad (\text{A-6})$$

the loading is now given by

$$(-\Delta C_p) = 4\alpha \tan \frac{\theta}{2} + 4\delta \left[ \frac{\chi}{\pi} \tan \frac{\theta}{2} + \frac{1}{\pi} \log \left| \frac{\sin (\theta + \chi)/2}{\sin (\theta - \chi)/2} \right| \right] \quad (\text{A-7})$$

where the final term gives rise to the logarithmic singularity at the flap hinge.

If now the chord ratio  $c_f/c$  is considered small, so that  $\sin \chi \approx \chi$ , then from (A-5)

$$\begin{aligned} C_L &= 2\pi\alpha + 2(\chi + \chi)\delta \\ &= 2\pi\alpha + 4\chi\delta \end{aligned} \quad (\text{A-8})$$

and the flap lift increment,  $\Delta C_{L_\delta}$ , is given by

$$\Delta C_{L_\delta} = 4\chi\delta \quad (\text{A-9})$$

Further the term

$$\frac{\sin (\theta + \chi)/2}{\sin (\theta - \chi)/2} ,$$

with, also  $\theta = \pi - 2\epsilon$ , becomes

$$\begin{aligned} \frac{\cos \left( \frac{\chi}{2} - \epsilon \right)}{\cos \left( \frac{\chi}{2} + \epsilon \right)} &= \frac{\cos \frac{\chi}{2} \cos \epsilon + \sin \frac{\chi}{2} \sin \epsilon}{\cos \frac{\chi}{2} \cos \epsilon - \sin \frac{\chi}{2} \sin \epsilon} \\ &\approx \frac{\left( 1 - \frac{\epsilon^2}{2} \right) \left( 1 - \frac{\chi^2}{4} \right) + \epsilon \frac{\chi}{2}}{\left( 1 - \frac{\epsilon^2}{2} \right) \left( 1 - \frac{\chi^2}{4} \right) - \epsilon \frac{\chi}{2}} \end{aligned}$$

which to the second order is unity. Hence close to the leading edge the logarithmic term does not contribute to the loading, which can now be written as

$$(-\Delta C_p) = \frac{4}{\epsilon} \left[ \alpha + \frac{\delta\chi}{\pi} \right] \quad (\text{A-10})$$

Hence at the position corresponding to  $\epsilon_s$ , the loading is given by

$$(-\Delta C_p) = \frac{4}{\epsilon_s} \left[ \alpha + \frac{\delta \chi}{\pi} \right] = \frac{2}{\pi} \frac{1}{\epsilon_s} [2\pi\alpha + 2\delta\chi]$$

and from (A-8) and (A-9), this may be written as

$$(-\Delta C_p) = \frac{2}{\pi} \frac{1}{\epsilon_s} \left[ C_L - \frac{\Delta C_{L\delta}}{2} \right].$$

Hence when  $(-\Delta C_p)$  reaches the critical value  $(-\Delta C_{ps})$

$$\left( -\Delta C_{ps} \right) = \frac{2}{\pi} \frac{1}{\epsilon_s} \left[ C_{L_{\max\delta}} - \frac{\Delta C_{L\delta}}{2} \right] \quad (\text{A-11})$$

and comparing with equation (A-4)

$$C_{L_{\max}} = C_{L_{\max\delta}} - \frac{\Delta C_{L\delta}}{2} \quad (\text{A-12})$$

where  $C_{L_{\max\delta}}$  is the maximum lift coefficient with the flap deflected. This result was first given by McRae<sup>21</sup>.

If it is now assumed that the flap is augmented by a jet of momentum coefficient  $C_{\mu}$ , again with a deflection  $\delta$ , Spence<sup>19</sup> gives the total lift coefficient (including the direct vertical momentum component of the jet) as

$$C_L = 2\pi(1 + 2B_0)\alpha + 2(\chi + \sin \chi + 2\pi D_0)\delta \quad (\text{A-13})$$

and the loading is

$$\begin{aligned} (-\Delta C_p) &= 4\alpha \tan \frac{\theta}{2} + 4\delta \frac{\chi}{\pi} \tan \frac{\theta}{2} + \frac{4\delta}{\pi} \log \left| \frac{\sin(\theta + \chi)/2}{\sin(\theta - \chi)/2} \right| \\ &+ 4x^{-3/2} \left\{ (\alpha B_0 + \delta D_0) \left( \frac{2X}{1-X} \right) + \sum_{n=1}^{\infty} (\alpha B_n + \delta D_n) X^n \right\} \end{aligned} \quad (\text{A-14})$$

where the coefficients  $B_n$  and  $D_n$  are related to the slope of the blowing jet, and to its momentum coefficient, and

$$X = \frac{1 - (1-x)^{1/2}}{1 + (1-x)^{1/2}}. \quad (\text{A-15})$$



Spence showed by a numerical example that only the leading coefficients  $B_0, B_1, D_0$  and  $D_1$  are significant. However in order to continue the analysis it is necessary to ignore all the coefficients except  $B_0$  and  $D_0$ . Because of this, the result finally obtained must be considered more approximate than that for plain flaps given in equation (A-12).

If, as before, it is assumed that  $\chi$  is small, equation (A-13) may be written as

$$C_L = 2\pi(1 + 2B_0)\alpha + 4(\chi + \pi D_0)\delta \quad .$$

Let

$$\Delta C_{L_{\delta, C_{\mu}}} = 2\pi \left[ 2B_0\alpha + \frac{2}{\pi}\chi\delta + 2D_0\delta \right] \quad (A-16)$$

be the lift increment due to flap deflection and the jet momentum, and

$$\Delta C_{L_{C_{\mu}}} = 2\pi[2B_0\alpha + 2D_0\delta] \quad (A-17)$$

be the lift increment due to the jet momentum at constant flap deflection.

As before, the contribution of the logarithmic term to the loading near to the leading edge will be assumed to be small.

The term

$$\frac{2X}{1-X} = \frac{2 \left\{ \frac{1 - (1-x)^{\frac{1}{2}}}{1 + (1-x)^{\frac{1}{2}}} \right\}}{\left\{ 1 - \frac{1 - (1-x)^{\frac{1}{2}}}{1 + (1-x)^{\frac{1}{2}}} \right\}} = \left\{ \frac{1}{(1-x)^{\frac{1}{2}}} - 1 \right\} \quad .$$

Substituting for  $\theta$  the term becomes

$$\left\{ \frac{1}{\sin \frac{\theta}{2}} - 1 \right\} \quad .$$

Hence for  $x^{-3/2} \left\{ \frac{2X}{1-X} \right\}$  the expression

$$\frac{1}{\cos^3 \frac{\theta}{2}} \left\{ \frac{1}{\sin \frac{\theta}{2}} - 1 \right\}$$

may be substituted, and close to the leading edge, the loading may be written as

$$(-\Delta C_p) = 4\alpha \tan \frac{\theta}{2} + 4\delta \frac{\chi}{\pi} \tan \frac{\theta}{2} + 4(\alpha B_0 + \delta D_0) \frac{1}{\cos^3 \frac{\theta}{2}} \left\{ \frac{1}{\sin \frac{\theta}{2}} - 1 \right\}$$

or

$$(-\Delta C_p) = 4 \tan \frac{\theta}{2} \left\{ \left[ \alpha + \frac{\delta \chi}{\pi} + \alpha B_0 + \delta D_0 \right] + [\alpha B_0 + \delta D_0] \left[ \frac{1}{\cos^3 \frac{\theta}{2}} \frac{1}{\tan \frac{\theta}{2}} \left\{ \frac{1}{\sin \frac{\theta}{2}} - 1 \right\} - 1 \right] \right\} .$$

Again, putting  $\theta = 2\pi - \epsilon$ , where  $\epsilon$  is small, the term

$$\frac{1}{\cos^3 \frac{\theta}{2}} \frac{1}{\tan \frac{\theta}{2}} \left\{ \frac{1}{\sin \frac{\theta}{2}} - 1 \right\} - 1 = \frac{1 - \sin \frac{\theta}{2}}{\sin^2 \frac{\theta}{2} \cos^2 \frac{\theta}{2}} - 1 = \frac{1 - \left[ 1 - \frac{\epsilon^2}{2} \right]}{\left[ 1 - \frac{\epsilon^2}{2} \right]^2 \frac{\epsilon^2}{2}} - 1$$

which to second order is

$$\frac{\frac{\epsilon^2}{2}}{\epsilon^2} - 1 = -\frac{1}{2} .$$

Hence  $(-\Delta C_p) = \frac{4}{\epsilon} \left\{ \left[ \alpha + \frac{\delta \chi}{\pi} + \alpha B_0 + \delta D_0 \right] - \frac{1}{2} [\alpha B_0 + \delta D_0] \right\}$  or, substituting from equations (A-13), (A-16) and (A-17)

$$(-\Delta C_p) = \frac{1}{\epsilon} \frac{2}{\pi} \left[ C_L - \frac{\Delta C_{L\delta, C_\mu}}{2} - \frac{\Delta C_{LC_\mu}}{4} \right] . \quad (A-18)$$

Thus when  $(-\Delta C_p)$  reaches the critical value  $(-\Delta C_{p_s})$

$$\left( -\Delta C_{p_s} \right) = \frac{2}{\pi} \frac{1}{\epsilon_s} \left[ C_{L_{\max}} - \frac{\Delta C_{L\delta, C_\mu}}{2} - \frac{\Delta C_{LC_\mu}}{4} \right] \quad (A-19)$$

and comparing with equation (A-4)

$$C_{L_{\max}} = C_{L_{\max, \delta, C_{\mu}}} - \frac{\Delta C_{L_{\delta, C_{\mu}}}}{2} - \frac{\Delta C_{L_C}}{4} \quad (A-20)$$

where  $C_{L_{\max, \delta, C_{\mu}}}$  is the maximum lift coefficient with the flap deflected and jet augmentation.

**Table 1**  
**MAIN FEATURES OF NASA TESTS ON EXTERNAL-FLOW JET FLAPS**

MACA/NASA paper	TN 3898	TN 4079	TN 4177	TN 4255	TN 4298	3-8-59L	5-1-59L	TN D-943	TN D-4278	TN D-4928	TN D-5129	TN D-5364	TN D-5408
Year	1956	1957	1958	1958	1958	1959	1959	1961	1967	1968	1969	1969	1969
Ref (present Report)	3	5	4	6	8	7	9	10	11	13	12	15	14
Tunnel	Langley 30ft x 60ft	Langley 7ft x 10ft	Langley 30ft x 60ft	Langley 30ft x 60ft	Langley 7ft x 10ft	Langley 30ft x 60ft	Langley 7ft x 10ft	Langley 30ft x 60ft	Ames 40ft x 80ft	Langley 30ft x 60ft	Ames 40ft x 80ft	Langley 30ft x 60ft	Langley 30ft x 60ft
Configuration tested	Wing and a/c	1/2 wing	a/c	a/c	a/c	a/c	1/2 a/c	a/c	a/c	a/c	a/c	a/c	a/c
Wing span	4 ft and 4.5 ft	2.5 ft	4.5 ft	6.8 ft	5.2 ft	6.8 ft	3.4 ft	32 ft	36 ft	12.5 ft	37.6 ft	8.3 ft	8 ft
Wing aspect ratio	6 and 6.6	6.0	6.6	6.6	3.0	6.6	7.0	6.5	5.4	7.8	6.5	7.0	7.8
Wing sweep ( $\pm$ c)	0° and 30°	0°	30°	30°	45°	30°	35°	35°	35°	25°	35°	8°	25°
Engine simulation								J69 Engines	J85 Engines	Model Fans	T58 Engines	Ejectors	Model Fans
Under (U) or Overwing (O)	U	U	U	U	O	U	O	U	U	U	U	U	U
Flap type	p and s	ds	s	s	ds	ds	p + vane	s	s + aux	ds	b/c + aux	ds + aux	ds
Flap span/wing span	1.0	1.0	1.0	0.67	0.75	1.0	0.6	1.0/0.55	0.63	0.75	0.67	0.75	0.75
Flap chord/wing chord	0.25	0.30	0.25	0.25	0.30	0.30	0.17	0.25	0.22	0.20	0.30	0.42	0.20
Leading-edge type	plain	plain	plain	plain	plain	plain	plain	plain	slat	slat	slat	slat	slat
Fish-tails fitted	no	no	no	no	yes	yes	yes	yes	no	no	no	no	no
Deflectors fitted	yes	yes	yes	yes	yes	yes	yes	yes	yes	no	yes	yes	no
Lateral tests	no	no	no	yes	no	no	no	no	yes	yes	no	yes	yes
Asymmetric tests	no	no	no	no	no	no	no	no	yes	yes	no	yes	yes

Notes. Configuration a/c = complete aircraft  
 Flap types p = plain, s = slotted, ds = double slotted, b/c = boundary layer control, aux = auxiliary flap.

SYMBOLS

A	aspect ratio	-
$C_A$	longitudinal force coefficient	-
$C_L$	lift coefficient	-
$C_{L_T}$	tail plane lift coefficient	-
$C_{L_0}$	lift coefficient at minimum drag	-
$C_{L_\Gamma}$	lift coefficient due to supercirculation	-
$(C_L)_{C_\mu=0}$	lift coefficient at zero jet momentum	-
$\Delta C_{L_{\delta, C_\mu}}$	increment in lift coefficient due to flap deflection and jet momentum	-
$\Delta C_L$	increment in lift coefficient due to jet momentum	-
$C_{D_0}$	profile drag coefficient	-
$\Delta C_{D_{Of}}$	increment in profile drag coefficient due to flaps	-
$C_\mu$	jet momentum coefficient (based on area S)	-
$C_{\mu_e}'$	jet momentum coefficient factored for losses and based on area S'	-
c	wing chord	m
F	factor accounting for finite aspect ratio (equation (2))	-
k	induced drag factor in equation (7)	-
$k_1$	incremental drag factor in equation (8)	-
$M_J$	mass flow in jet	kg/sec
$q_0$	free stream dynamic pressure	$N/m^2$
r	thrust recovery factor	-
S	wing area	$m^2$
S'	wing area affected by jet flap	$m^2$
t	wing thickness	m
$V_J$	velocity of jet	m/sec
$\alpha$	angle of incidence	rad
$\delta_J$	effective jet deflection angle	rad or deg

SYMBOLS (Contd) .

$\epsilon$	downwash angle	rad	2
$\eta$	static turning efficiency	-	
$\theta$	jet deflection angle ( $\equiv \delta_J$ )	rad	3
$\lambda$	part span factor for lift (equation (3))	-	
$\nu$	part span factor for lift (equation (4))	-	

REFERENCES

- | <u>No.</u> | <u>Author(s)</u>                             | <u>Title, etc.</u>   |
|------------|--|--|
| 1          | J. Williams<br>S. F. J. Butler<br>M. N. Wood | The aerodynamics of jet flaps:<br>ARC R & M 3304 (1961)  |
| 2          | K. D. Harris                                 | The Hunting H 126 jet-flap research aircraft.<br>In <i>Assessment of lift augmentation schemes</i> ,<br>edited by J. Williams and P. Colin<br>AGARDOGRAPH (to be published)  |
| 3          | J. P. Campbell<br>J. L. Johnson              | Wind-tunnel investigation of an external-flow<br>jet-augmented slotted flap suitable for<br>application to airplanes with pod-mounted<br>engines.<br>NACA TN 3898 (1956)   |
| 4          | J. L. Johnson                                | Wind-tunnel investigation of the static<br>longitudinal stability and trim characteristics<br>of a sweptback wing jet transport model equipped<br>with an external-flow jet-augmented flap.<br>NACA TN 4177 (1958) |
| 5          | E. E. Davenport                              | Wind-tunnel investigation of external-flow jet-<br>augmented double-slotted flaps on a rectangular<br>wing at an angle of attack of $0^{\circ}$ to high<br>momentum coefficients.<br>NACA TN 4079 (1957)           |
| 6          | J. L. Johnson                                | Wind-tunnel investigation at low speeds of flight<br>characteristics of a sweptback wing jet transport<br>airplane model equipped with an external-flow jet-<br>augmented slotted flap.<br>NACA TN 4255 (1958)     |
| 7          | J. L. Johnson                                | Wind-tunnel investigation of a small scale<br>sweptback wing jet transport model equipped with<br>an external-flow jet-augmented double slotted<br>flap.<br>NASA Memorandum 3-8-59L (1959)                         |

REFERENCES (Contd)

<u>No.</u>	<u>Author(s)</u>	<u>Title, etc.</u>
8	J. M. Riebe E. E. Davenport	Exploratory wind-tunnel investigation to determine the lift effects of blowing over flaps from nacelles mounted above the wing. NACA TN 4298 (1958)
9	T. R. Turner E. E. Davenport J. M. Riebe	Low speed investigation of blowing from nacelles mounted inboard and on the upper surface of an aspect ratio 7.0 35° swept wing with fuselage and various tail arrangements. NASA Memorandum 5-1-59L (1959)
10	M. P. Fink	Aerodynamic characteristics, temperature and noise measurements on a large scale external-flow jet-augmented flap model with turbojet engines operating. NASA TN D-943 (1961)
11	J. V. Kirk D. H. Hickey Kiyoshi Aoyagi	Large scale wind-tunnel investigation of a model with an external jet-augmented flap. NASA TN D-4278 (1967)
12	Kiyoshi Aoyagi S. O. Dickinson P. T. Soderman	Investigation of a 0.3 scale jet transport model having a jet-augmented boundary layer control flap with direct lift control capability. NASA TN D-5129 (1969)
13	L. P. Parlett M. P. Fink D. C. Freeman	Wind-tunnel investigation of a large jet transport model equipped with an external-flow jet flap. NASA TN D-4928 (1968)
14	D. C. Freeman S. B. Grafton R. D'Amato	Static and dynamic stability derivatives of a model of a jet transport equipped with external-flow jet-augmented flaps. NASA TN D-5408 (1969)
15	L. P. Parlett J. P. Shivers	Wind-tunnel investigation of an STOL aircraft configuration equipped with an external-flow jet flap. NASA TN D-5364 (1969)

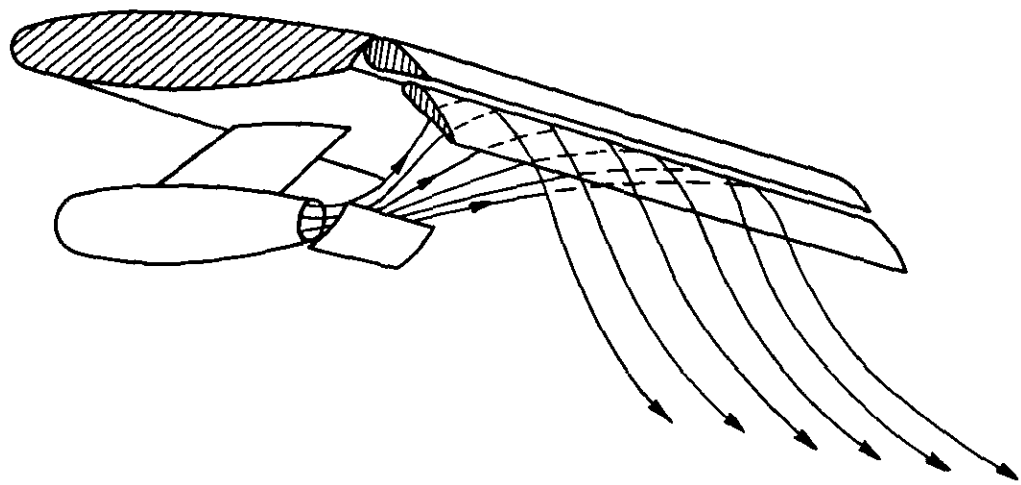


REFERENCES (Contd)

<u>No.</u>	<u>Author(s)</u>	<u>Title, etc.</u>
16	P. F. Ashwood D. Lean	Flight tests of a Meteor aeroplane fitted with jet deflection. J. R. Ae.Soc., Vol.62, No.572 (1958)
17	G. L. Wilde	Jet lift engines and power plants for VTOL aircraft. J. R. Ae.Soc., Vol.65, No.609 (1961)
18	D. A. Spence	A treatment of the jet flap by thin aerofoil theory. RAE Report Aero 2568 (ARC 18472) (1955)
19	D. A. Spence	The lift on a thin aerofoil with a <b>blown</b> flap. Ae. Quart., Vol.9, pt.3, pp.287-299 RAE Technical Note 2450 (ARC 18473) (1956)
20	E. C. Maskell D. A. Spence	A theory of the jet flap in three dimensions. Proc. Roy. Soc., A, Vol.251, pp.407-425 (1959) RAE Report 2612 (ARC 20744) (1958)
21	D. M. McRae	The aerodynamics of high-lift devices on conventional aircraft Part 1. J. R. Ae.Soc., Vol.73, No.702, pp.535-541 (1969)
22	-	The low-speed stalling characteristics of aerodynamically smooth aerofoils. R. Ae.Soc., Engineering Sciences Data Unit, Item No.66034, Issue 1 (1956)
23	H. R. Hopkin	A scheme of notation and nomenclature for aircraft dynamics and associated aerodynamics. (ARC R & M 3562) (1966)
24	A. O. Wood	Revised performance estimates for the H 126 jet-flap research aeroplane. Hunting Aircraft Ltd. Report AERO 126/41 (1963)

REFERENCES (Contd)

<u>No.</u>	<u>Author(s)</u>	<u>Title, etc.</u>
25	A. J. Ross	The theoretical evaluation of the downwash behind jet-flapped wings. ARC R & M 3119 (1958)
26	C. R. Taylor	Flight test results of a trailing-edge flap designed for direct-lift control. NASA CR-1426 (1969)
27	D. E. Morris J. C. Morrall	Effect of slipstream on longitudinal stability of multi-engined aircraft. ARC R & M 2701 (1948)
28	D. J. Maglieri H. H. Hubbard	Preliminary measurements of the noise characteristics of some jet-augmented flap configurations. NASA Memorandum 12-4-58L (1959)
29	H. Multhopp	On the maximum lift coefficient of aerofoil sections. ARC 12115 (1948)
30	J. Weber	The calculation of the pressure distribution over the surface of two-dimensional and swept wings with symmetrical aerofoil sections. (ARC R & M 2918) (1953)



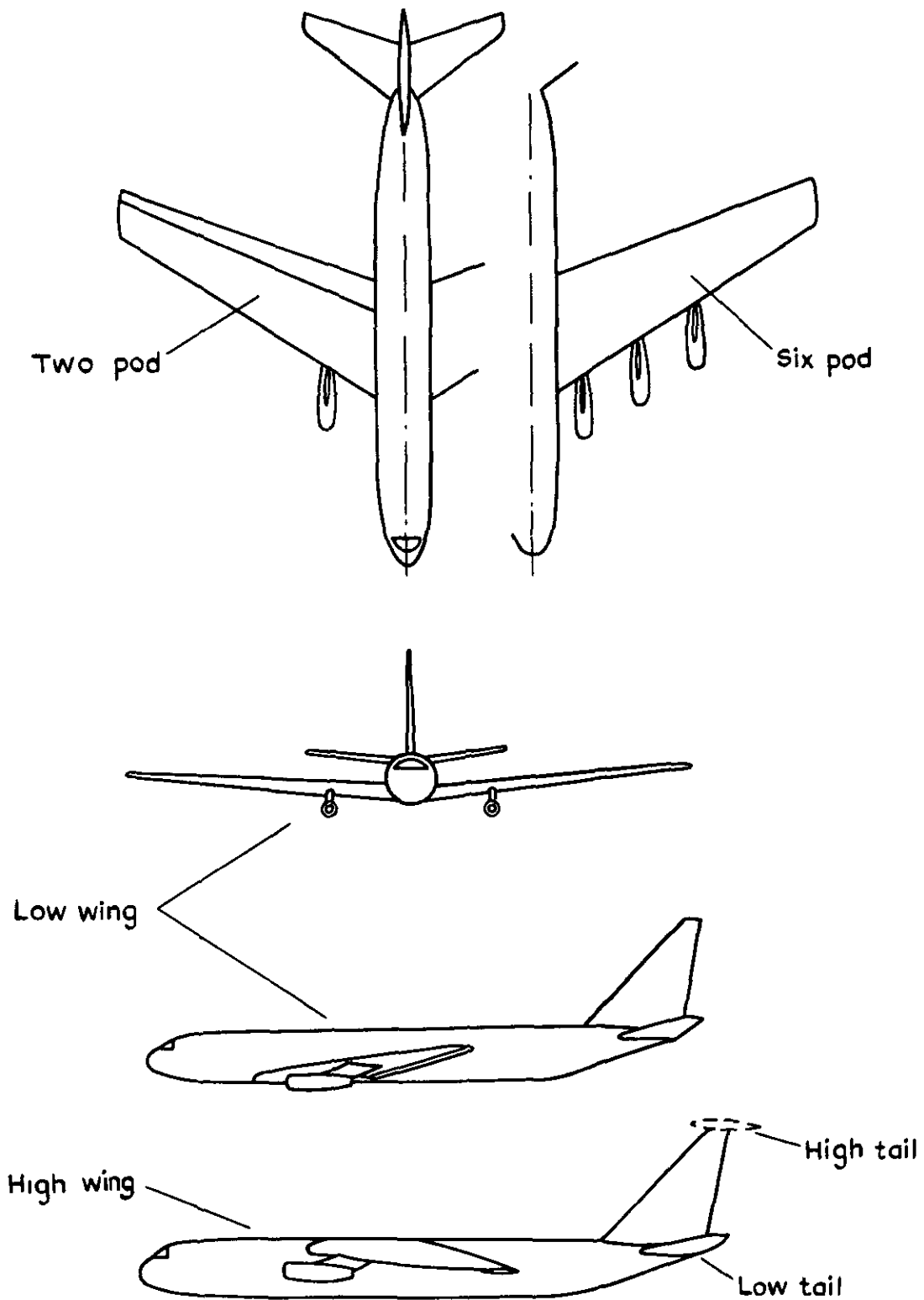


Fig.2 Some of the configurations tested in NACA TN 3898  
and 4177 (Refs 3 & 4)

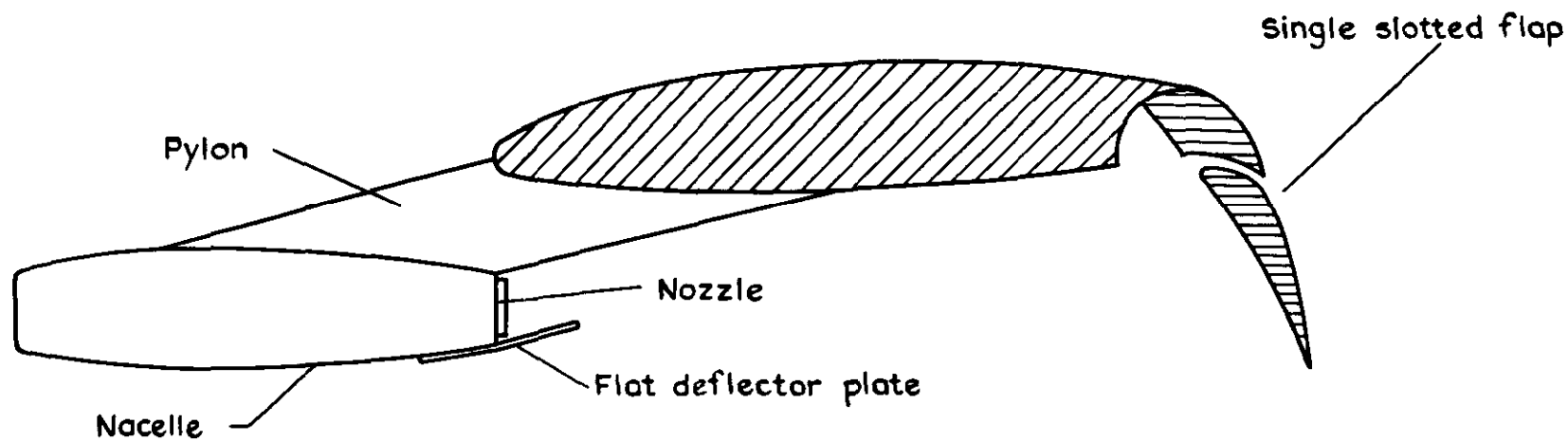


Fig.3 Arrangement of nozzle , deflector plate and flap, tested in  
NACA TN 3898 and 4177 (Refs 3&4)

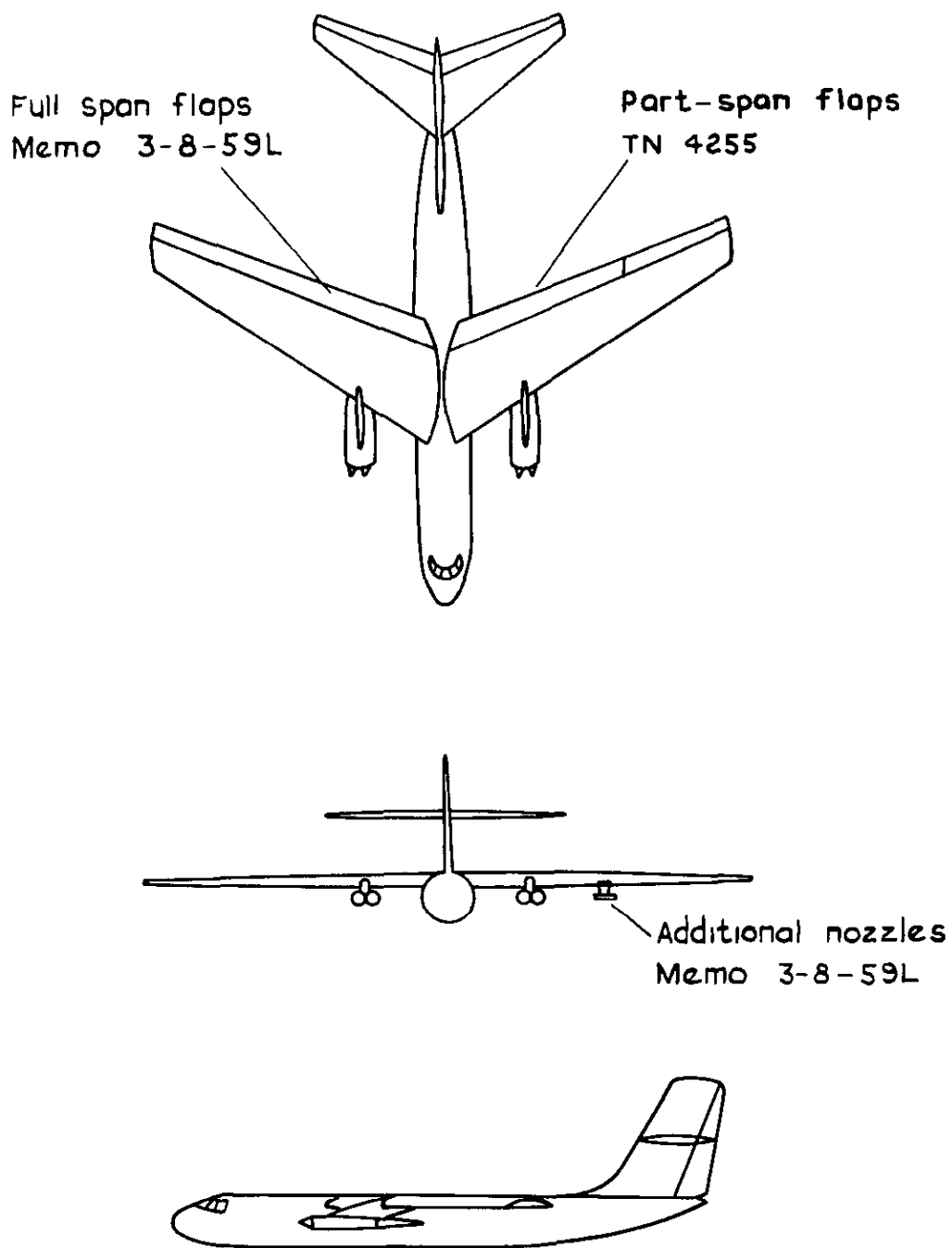
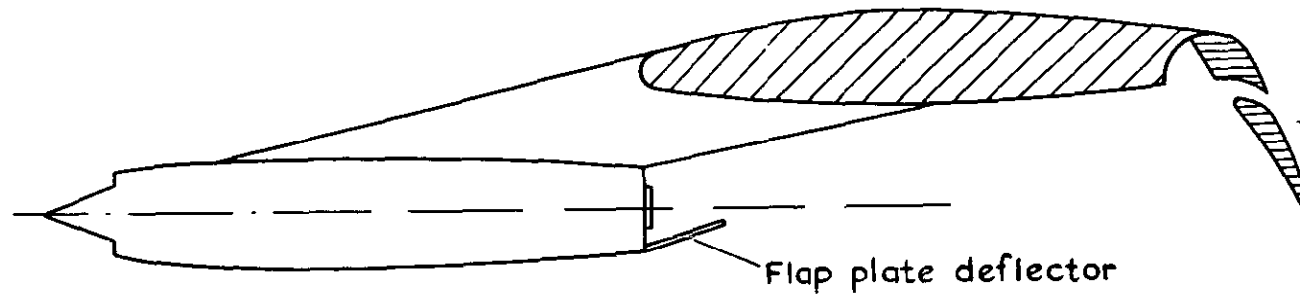
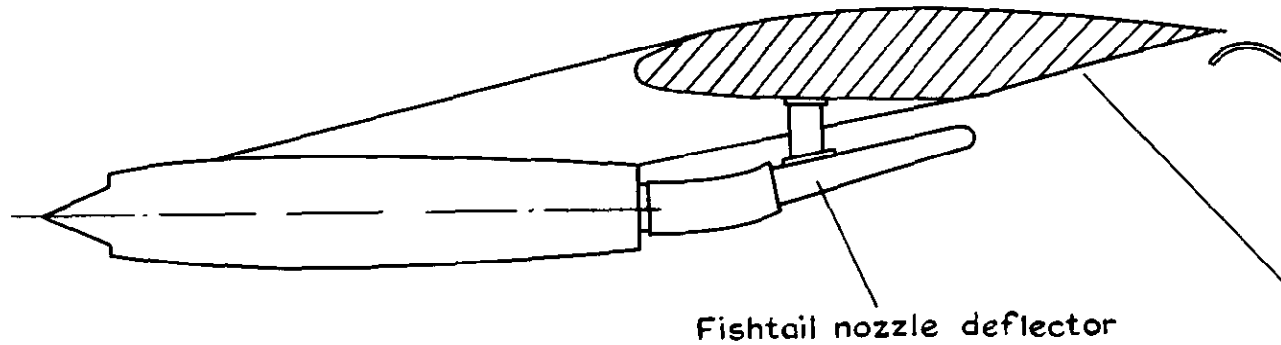


Fig 4 Some of the configurations tested in NACA TN 4255 and NASA Memo 3-8-59L (Refs 6 & 7)



a NACA TN 4255



b NASA Memo 3-8-59L

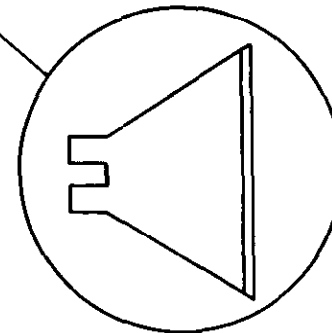


Fig.5 a & b Arrangement of nozzle, deflectors and flaps tested in  
NASA Memo 3-8-59L (Refs 6 & 7)

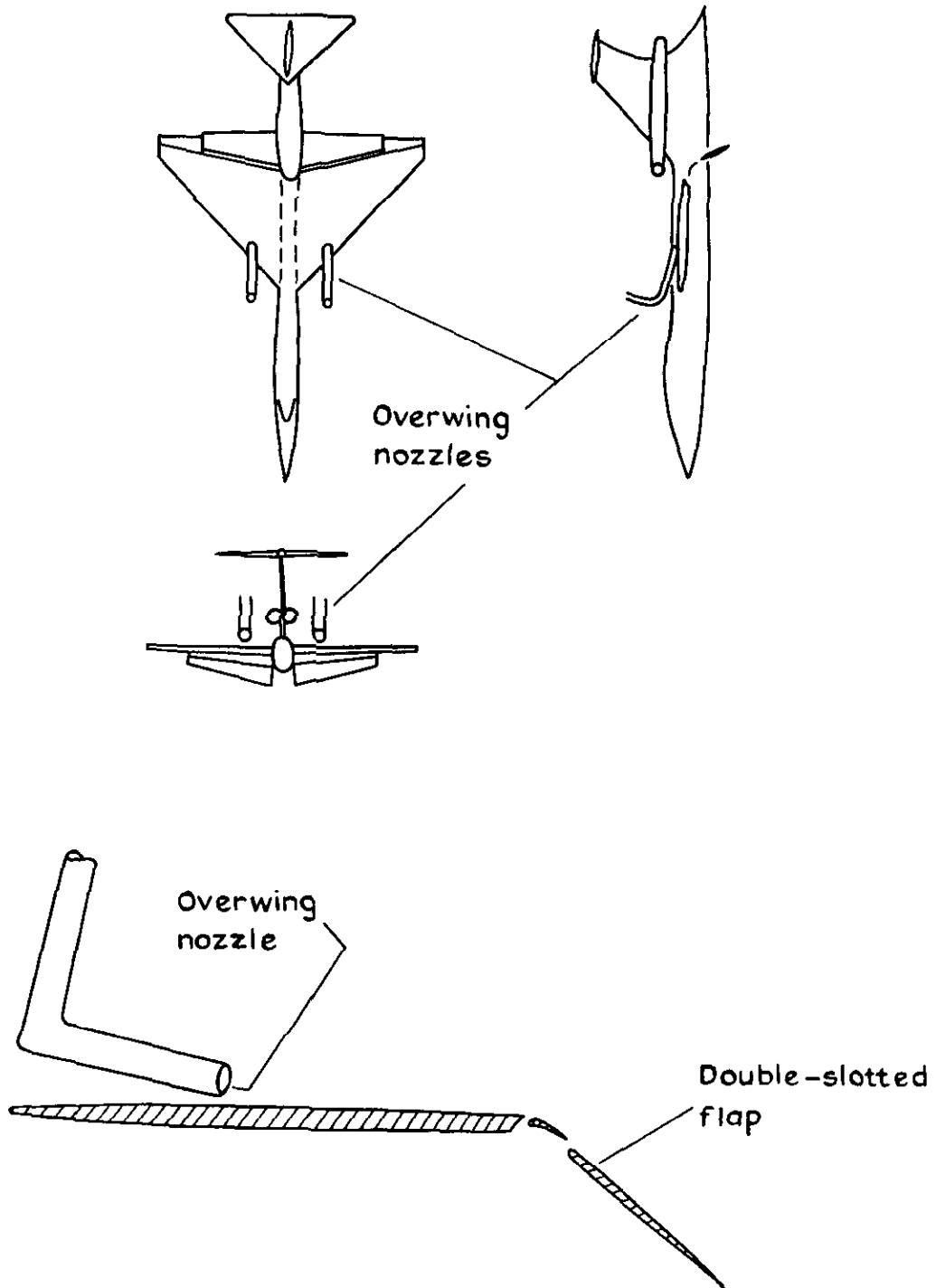


Fig-6 Configuration tested in NACA TN 4298 (Ref 8)



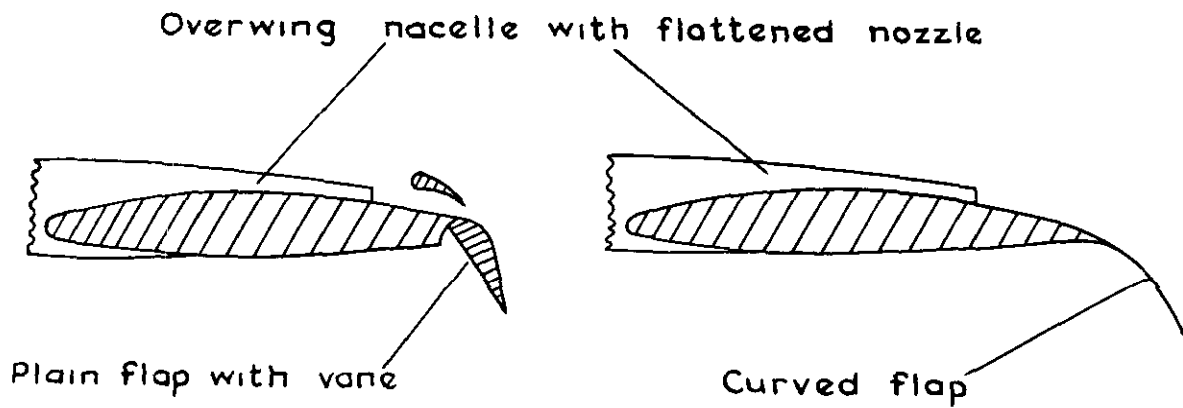
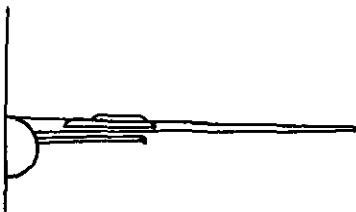
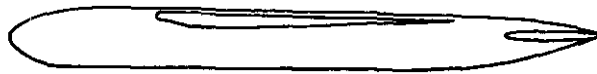
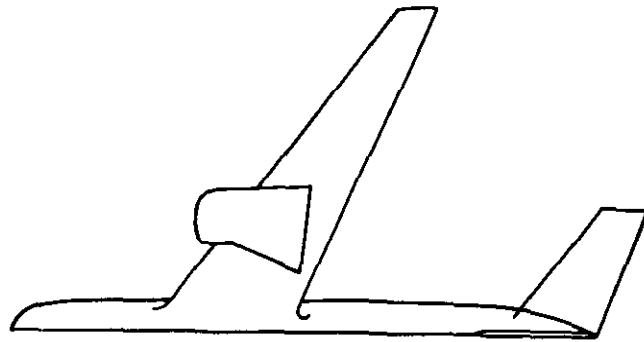


Fig.7 Some configurations tested in NASA Memo 5-1-59L (Ref 9)

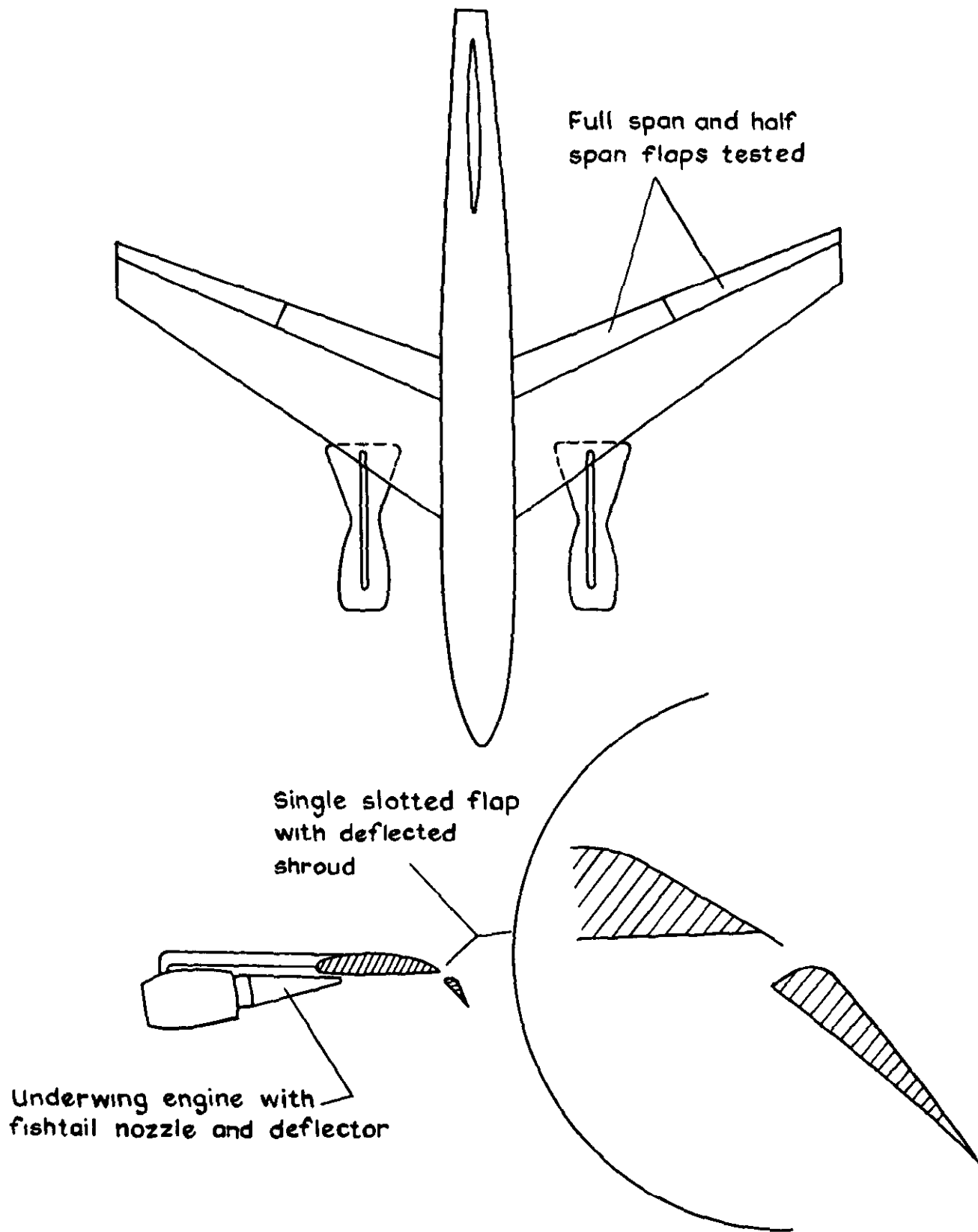
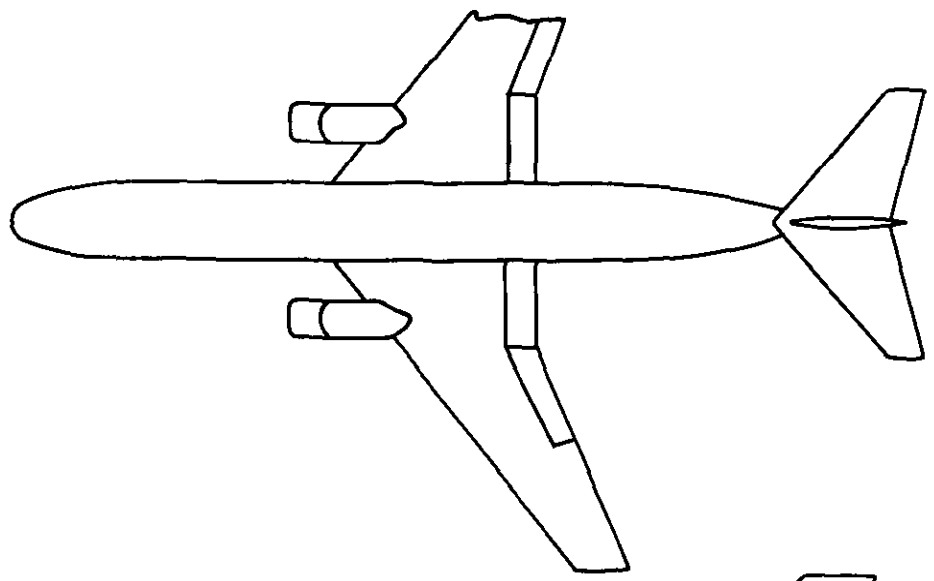
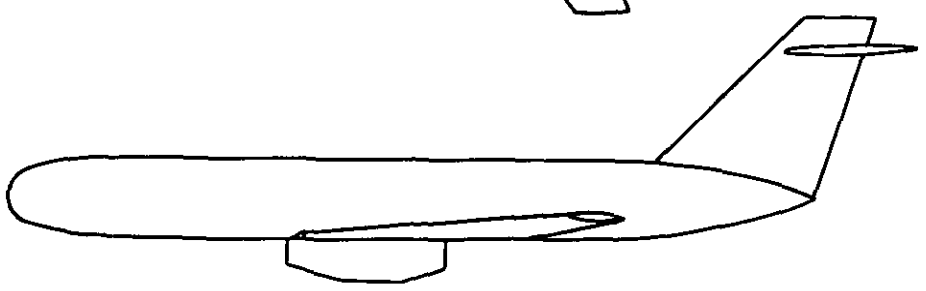


Fig.8 Configuration tested in NASA TN D-943 (Ref 10)

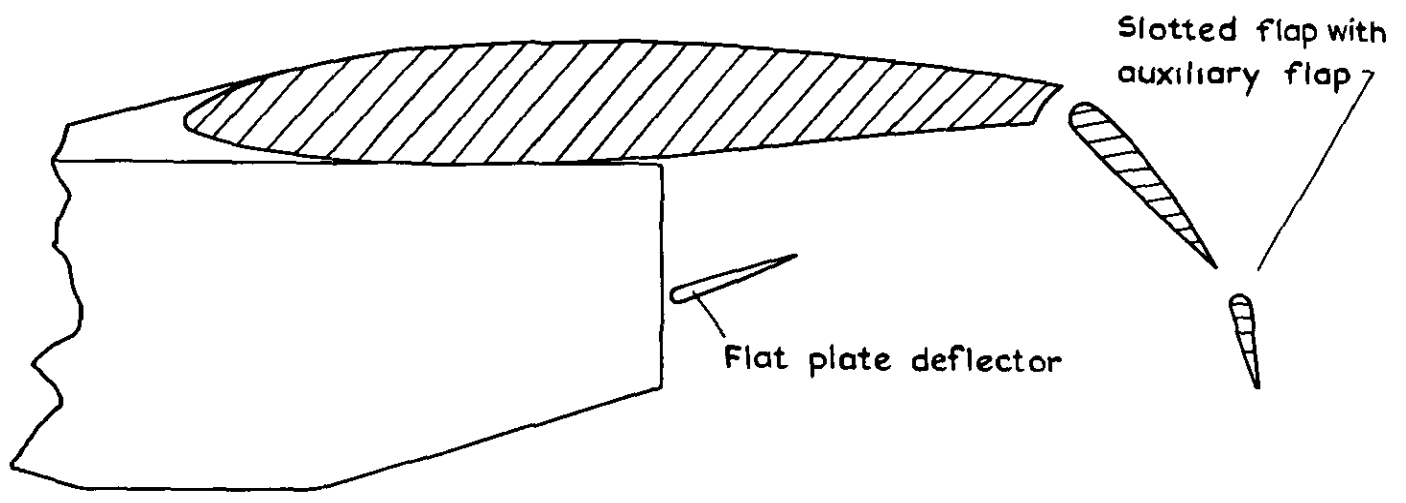
2)



3)



•



•

•

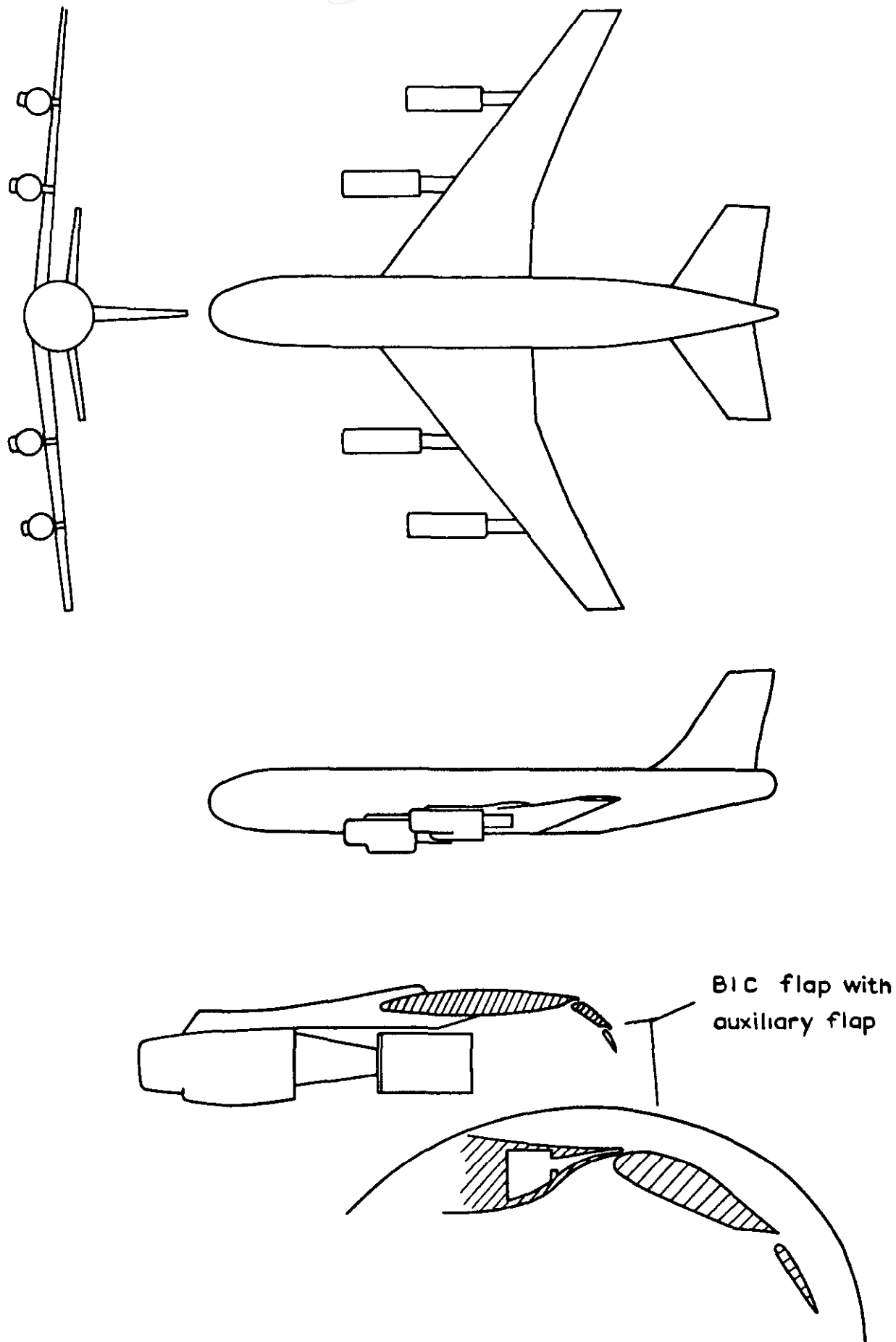


Fig.10 Configuration tested in NASA TN D-5129 (Ref 12)

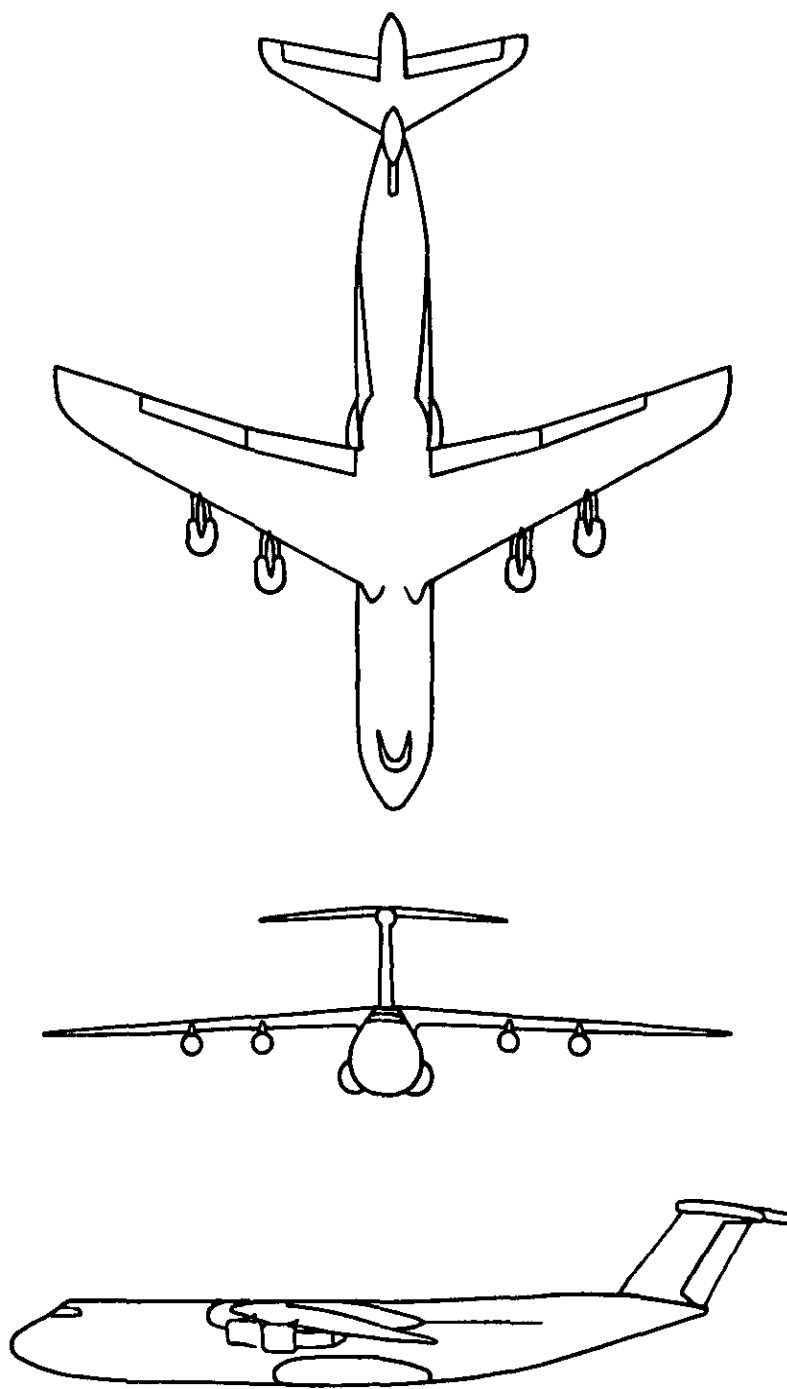


Fig.II Configuration tested in NASA TND-4928  
and D-5408 (Refs 13&14)

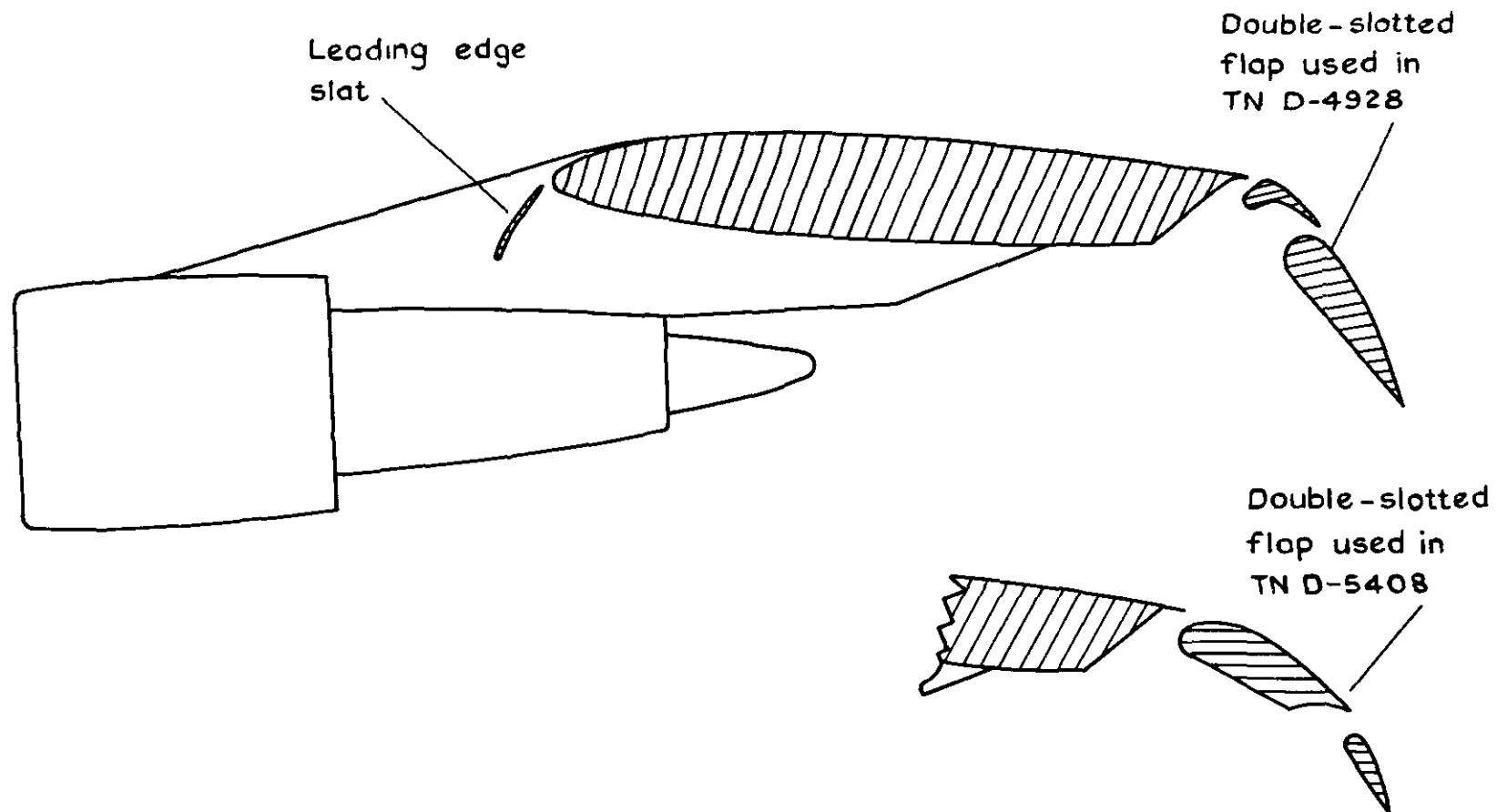
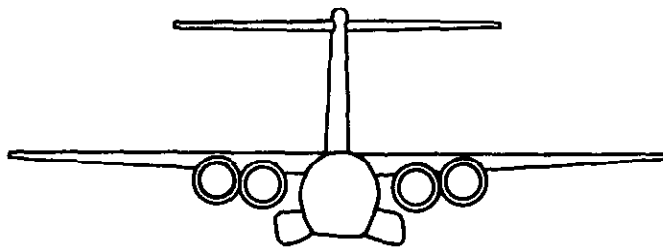
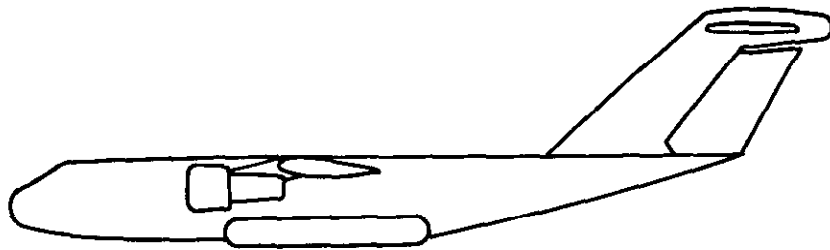
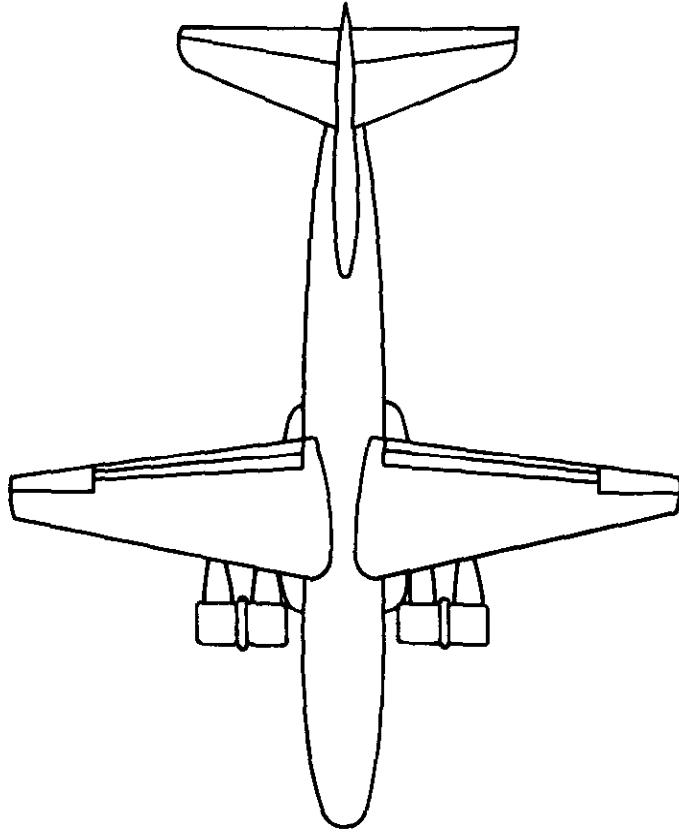


Fig.12 Arrangement of nozzle and flaps tested in  
NASA TN D-4928 and D-5408 (Refs 13 & 14)



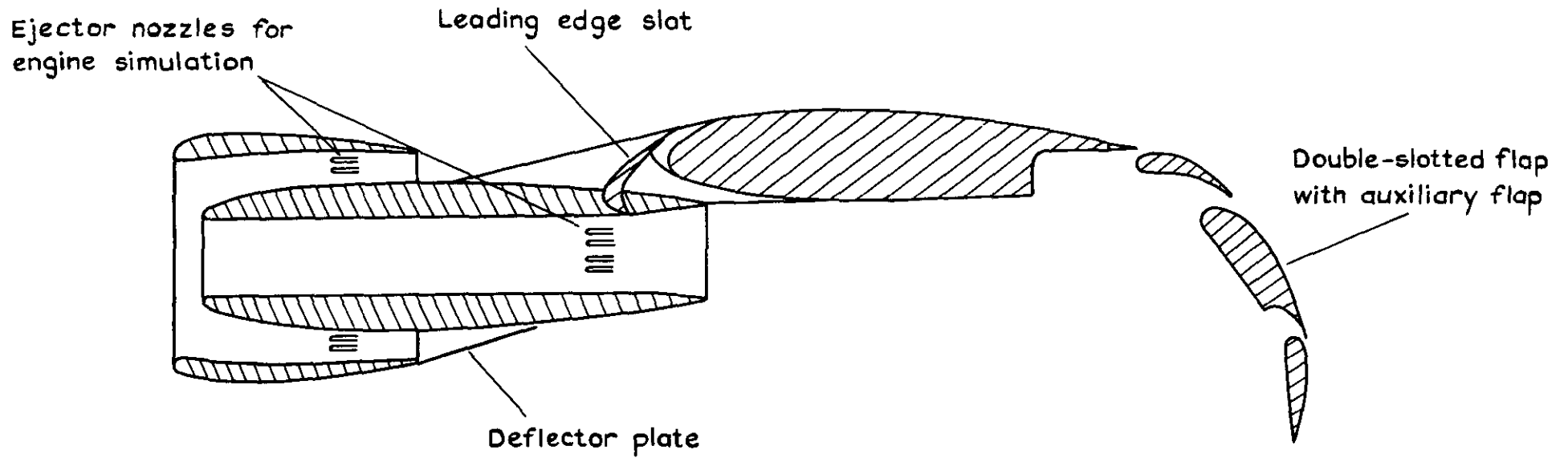


Fig. 14 Arrangement of nozzles, deflector and flap tested in NASA TN 5364 (Ref 15)



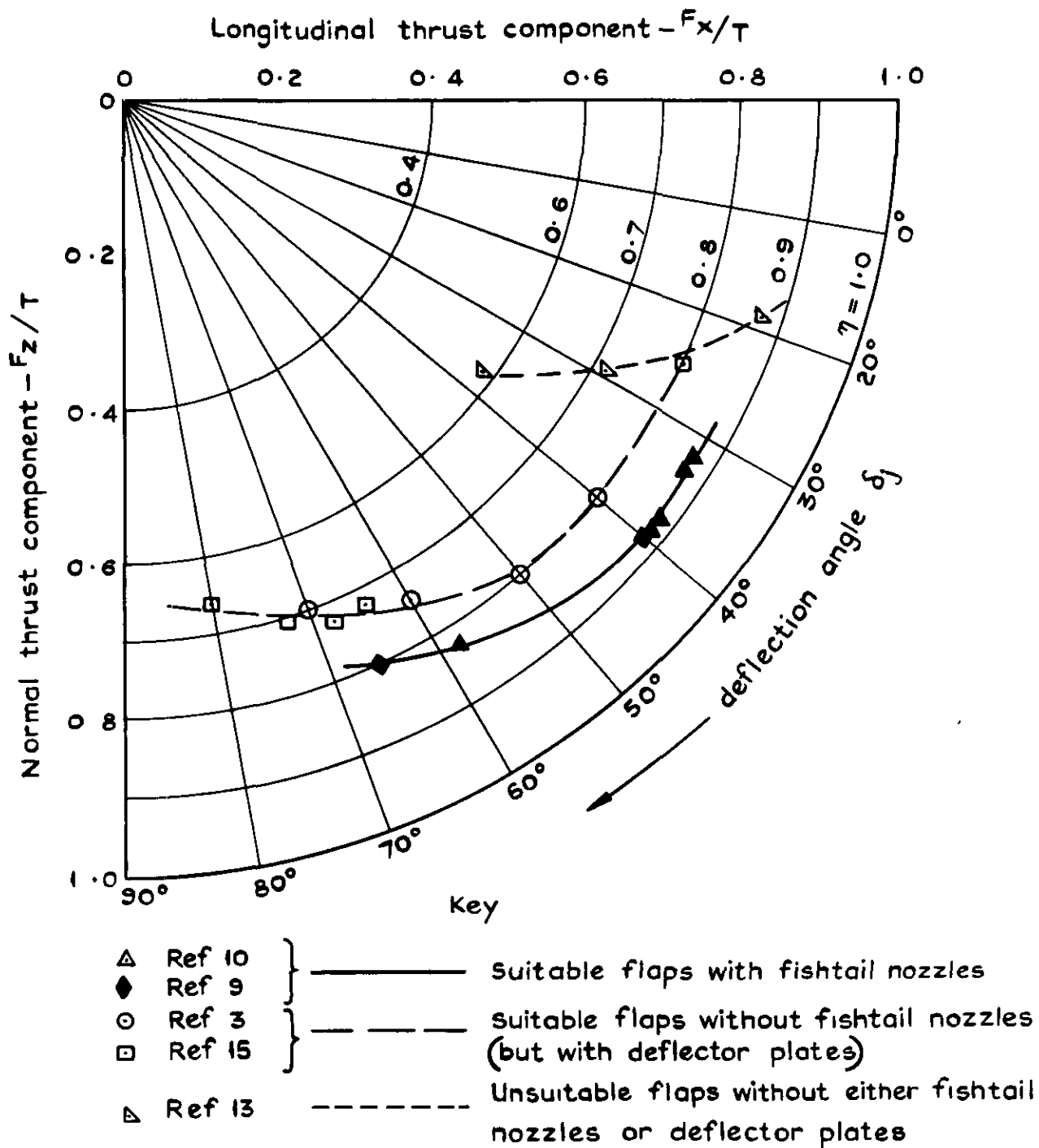
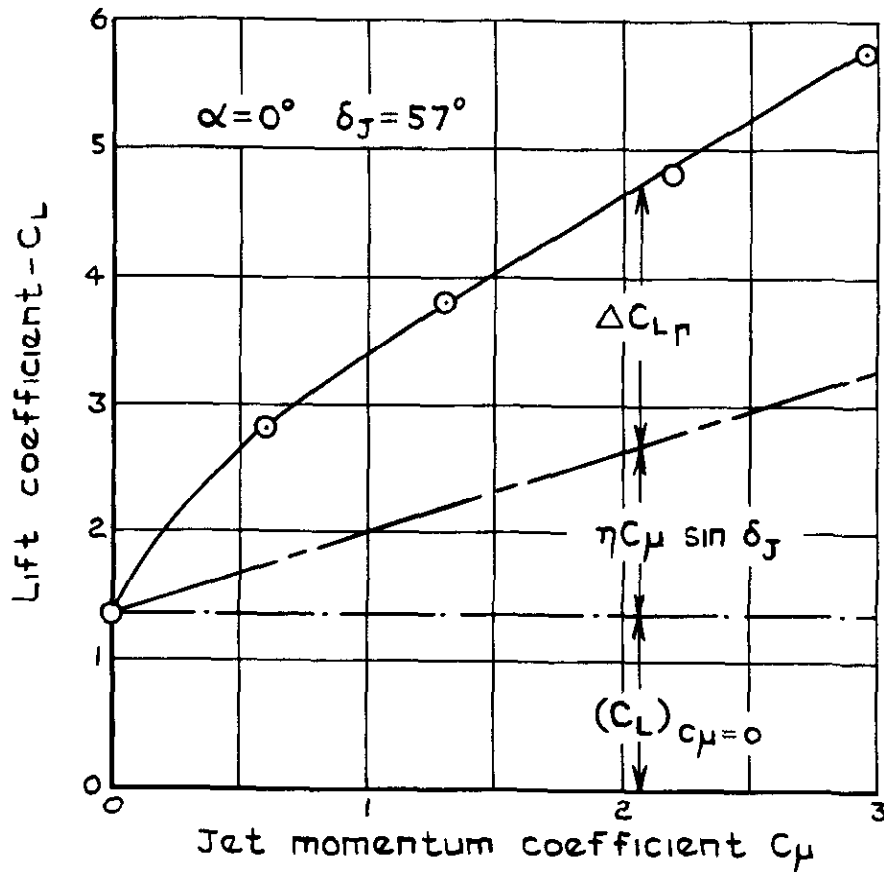
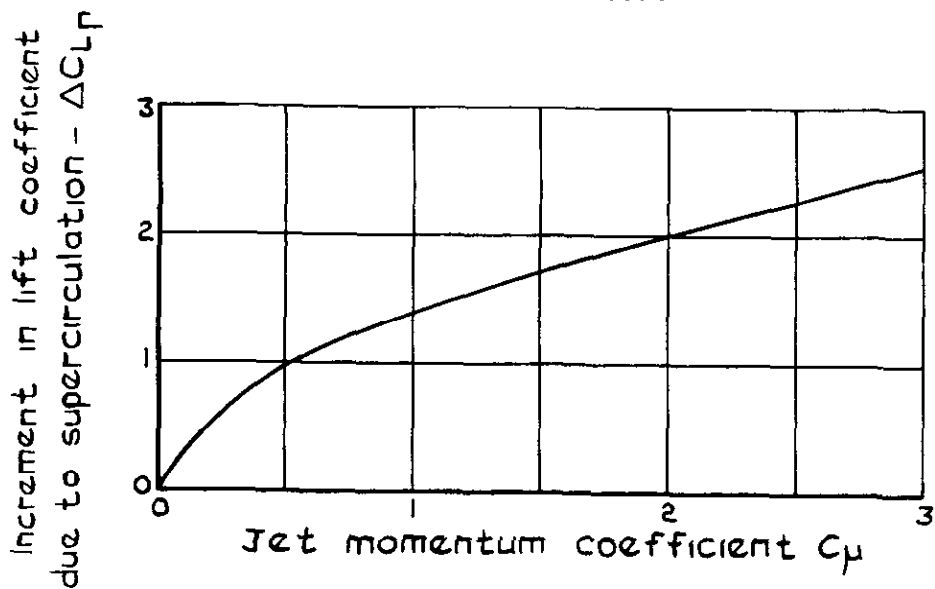


Fig.15 Static turning efficiency for some configurations with under-wing jet-augmented flaps



a Overall lift



b Supercirculation lift

Fig 16a & b Typical variation of lift coefficient with jet momentum coefficient (data from Ref 7)

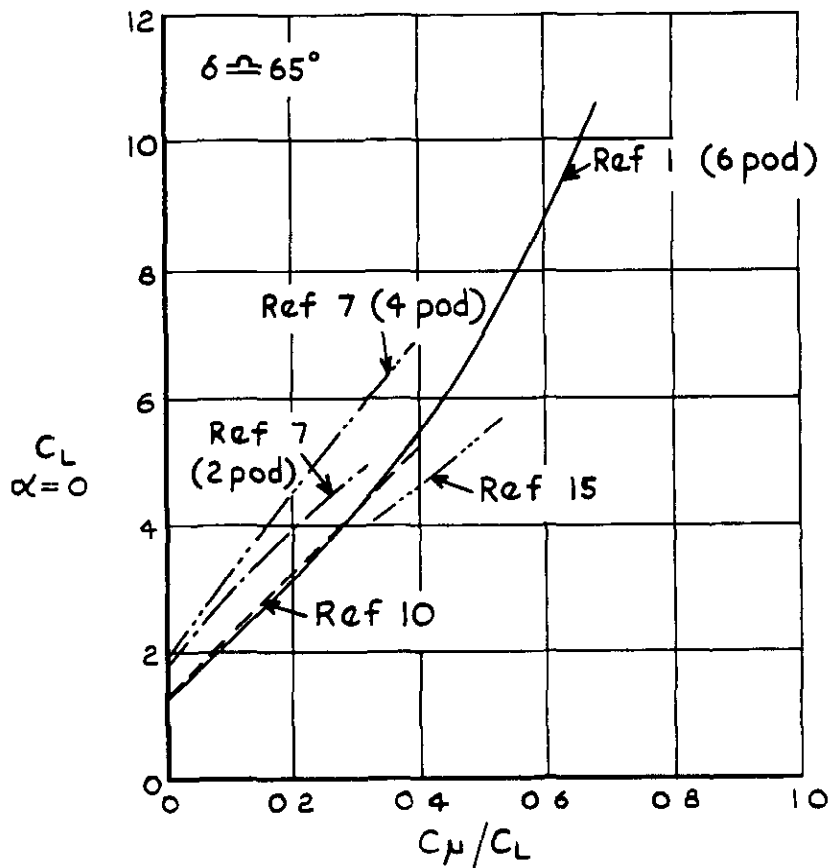
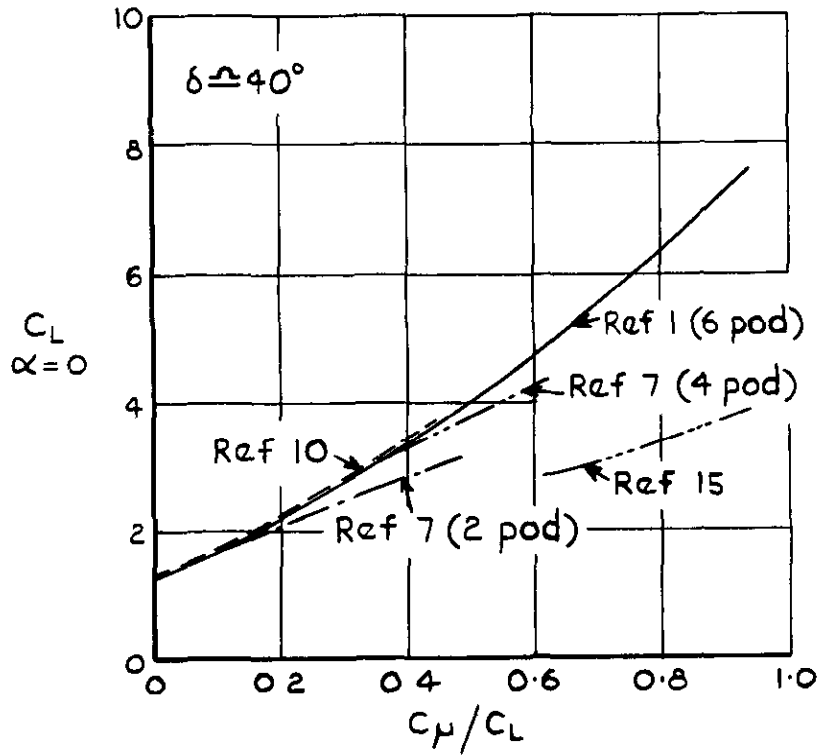


Fig. 17. Lift coefficients at zero incidence from

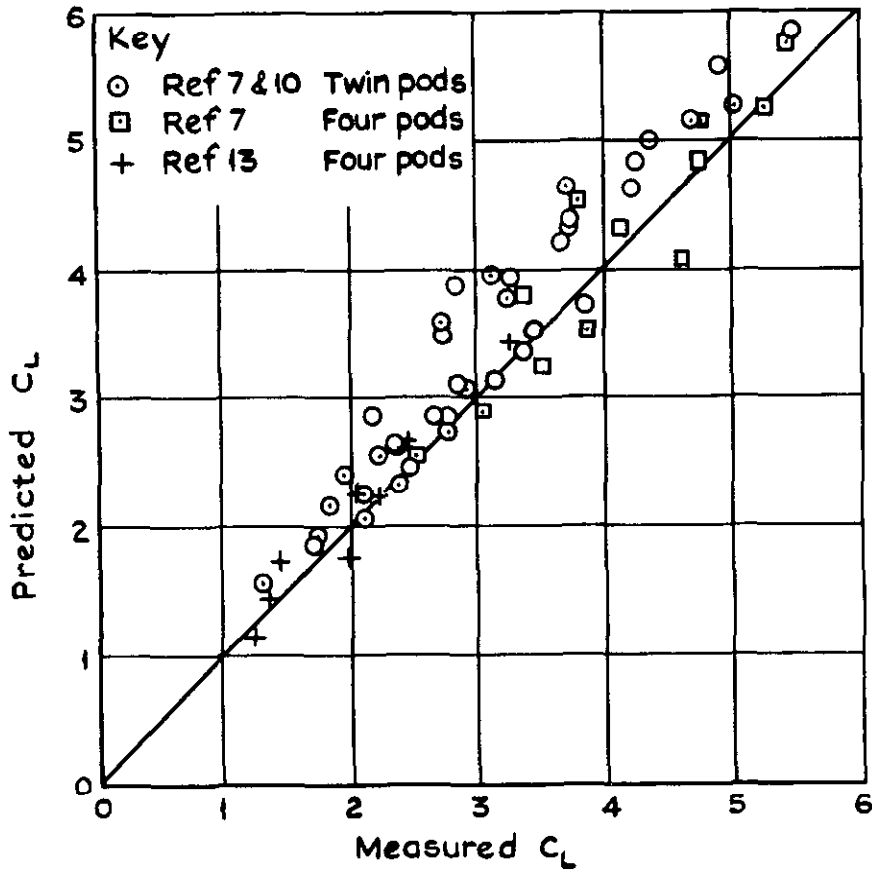


Fig.18 Comparison of measured  $C_L$ 's with those predicted by equation (1)

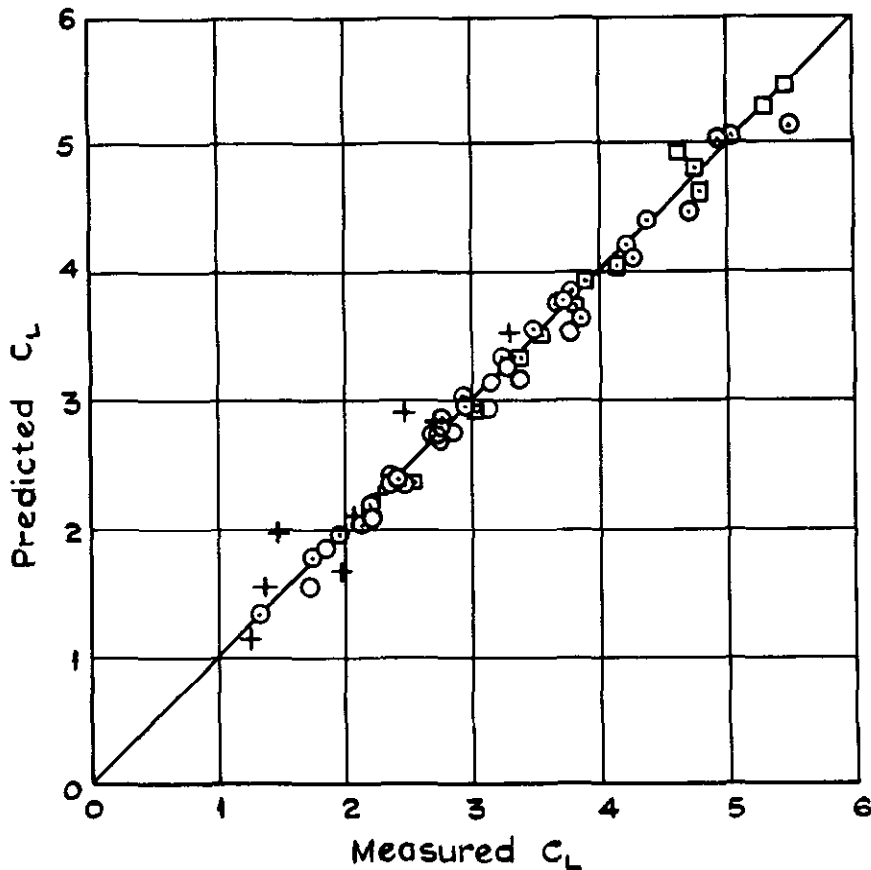
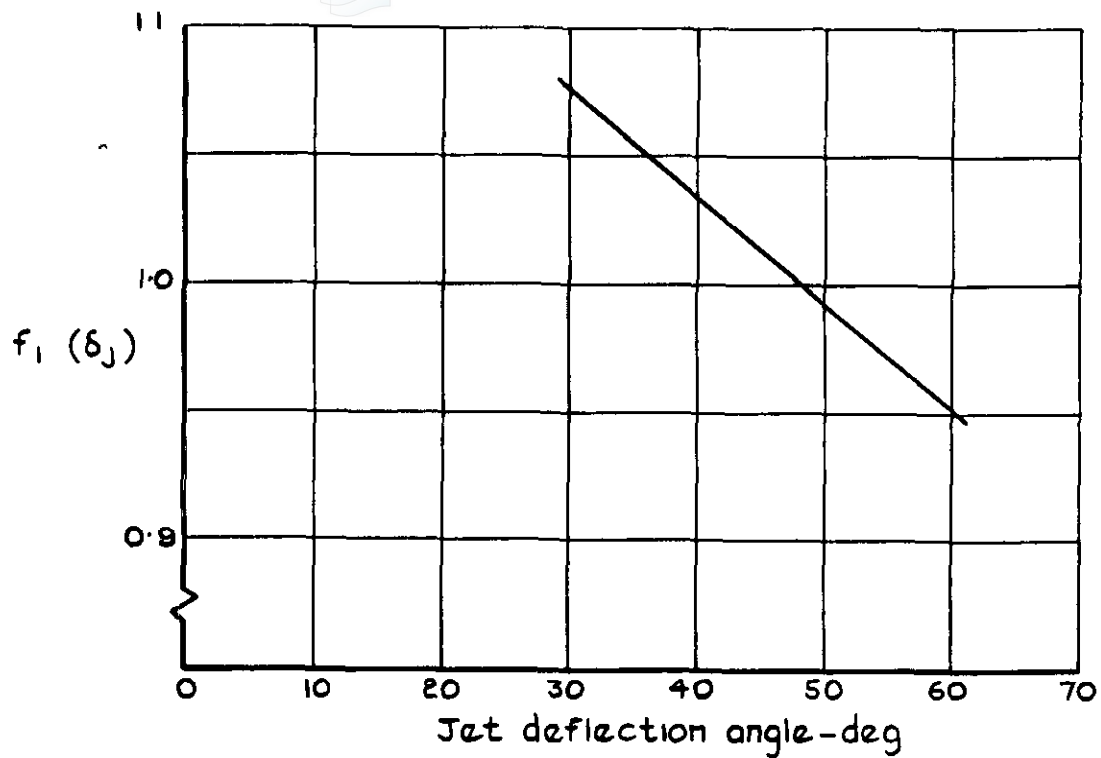
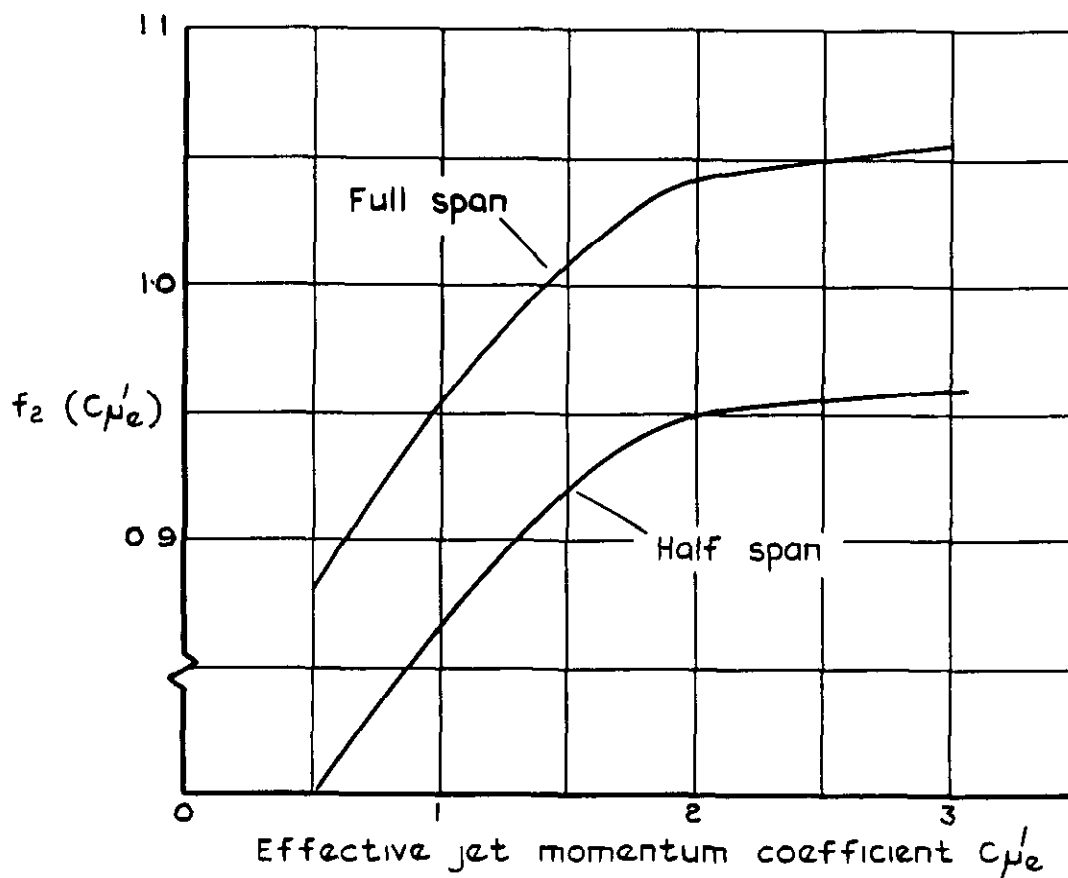


Fig.19 Comparison of measured  $C_L$ 's with those predicted by equation (1), modified by empirical factors

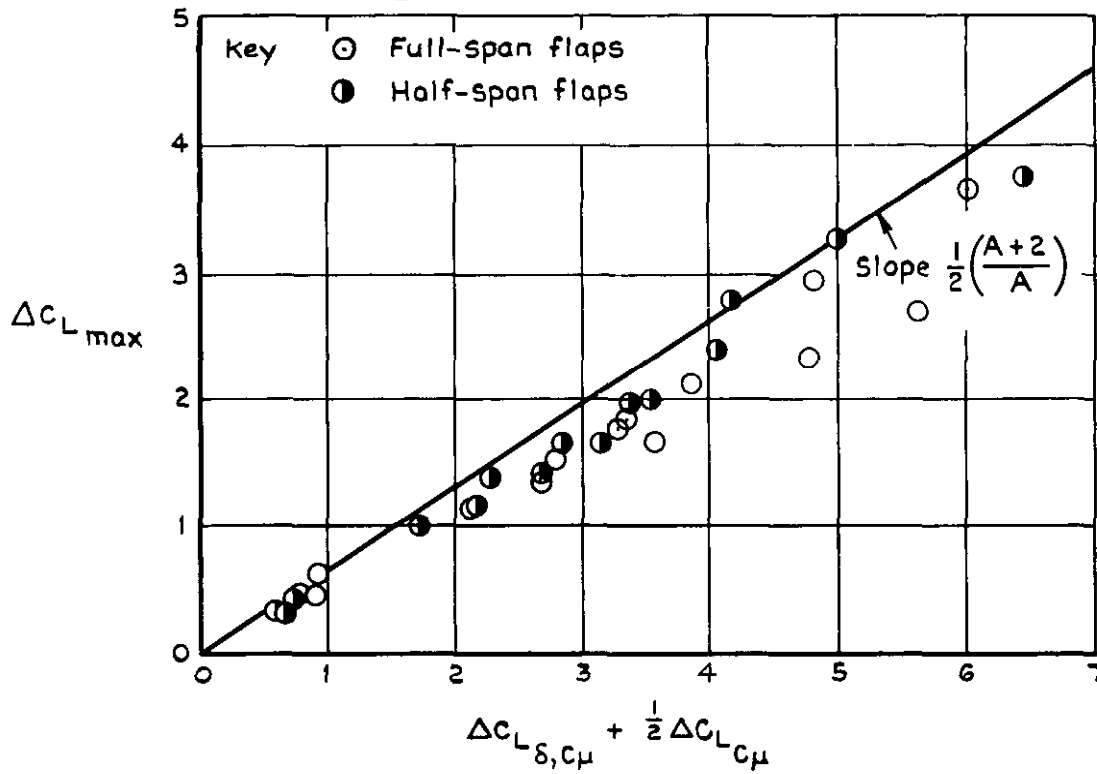


a

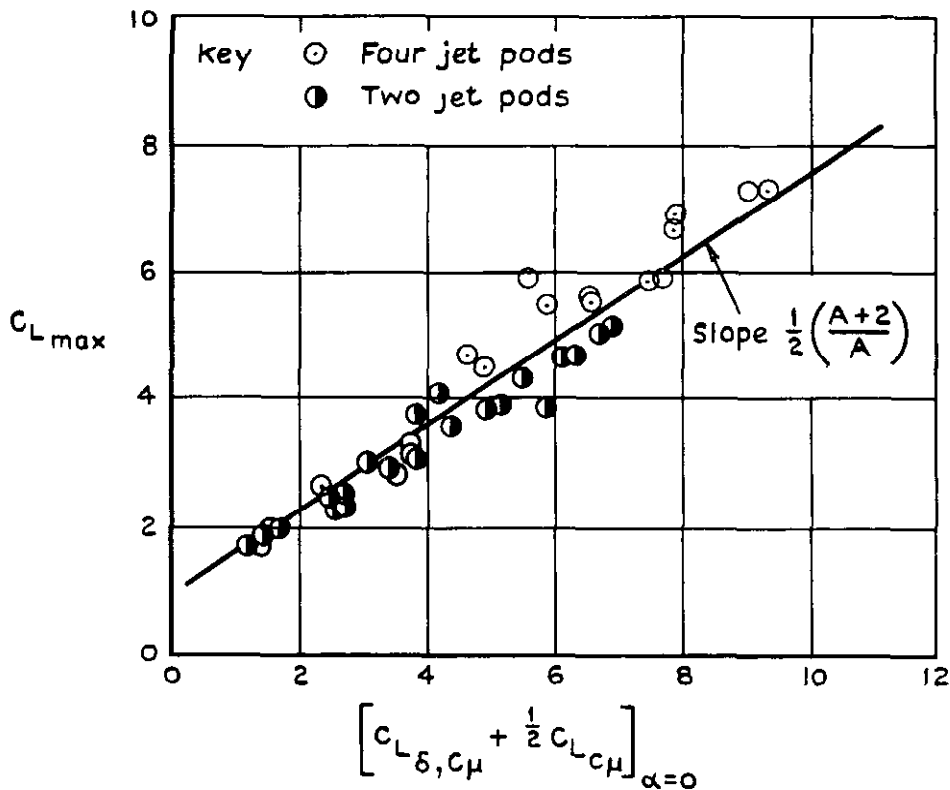


b

Fig.20 a&b Empirical correction factors to lift coefficients predicted by equation (1)

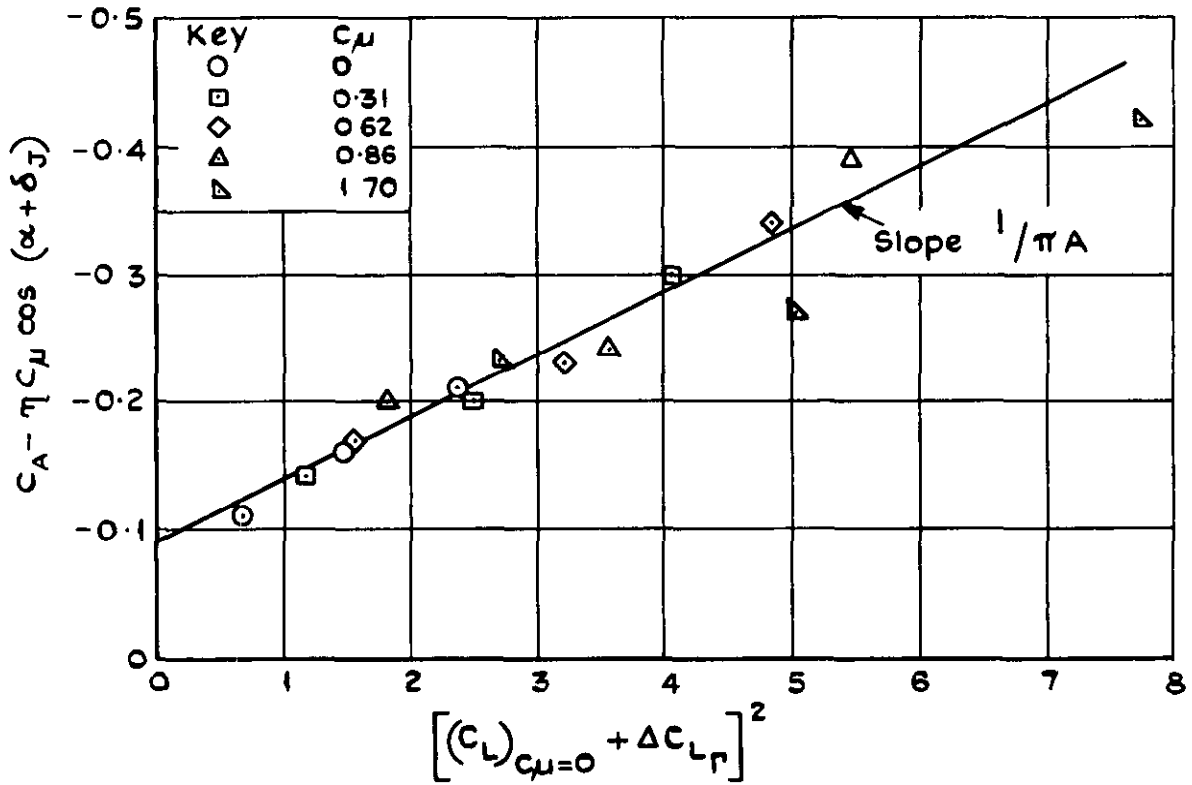


a Data from NASA TN D 943 (Ref 10)

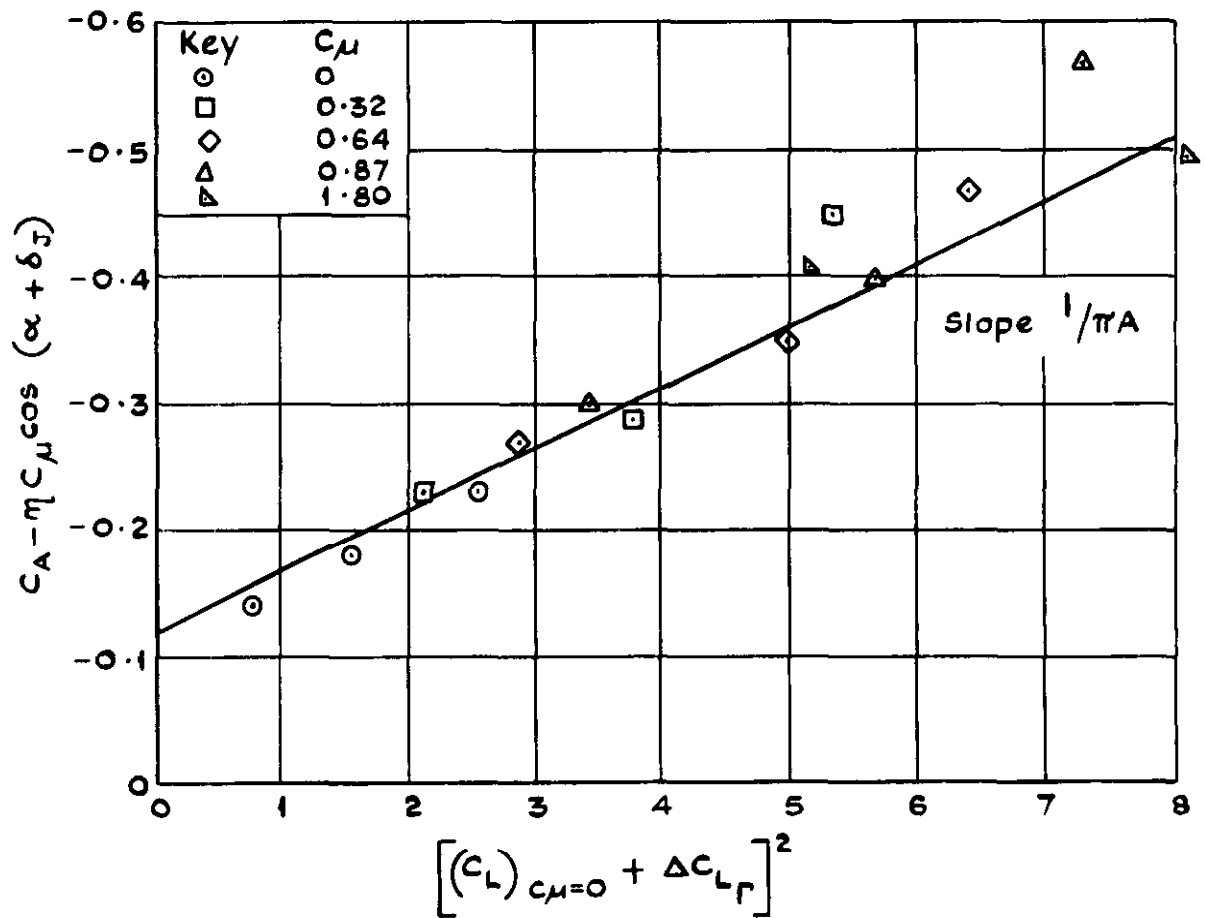


b Data from NASA Memo 3-8-59L (Ref 7)

Fig.21a&b Maximum lift coefficients for external flow jet flaps



a Flap angle  $30^\circ$



b Flap angle  $40^\circ$

Fig. 22 Analysis of longitudinal force data from NASA TN D943 (Ref 10)

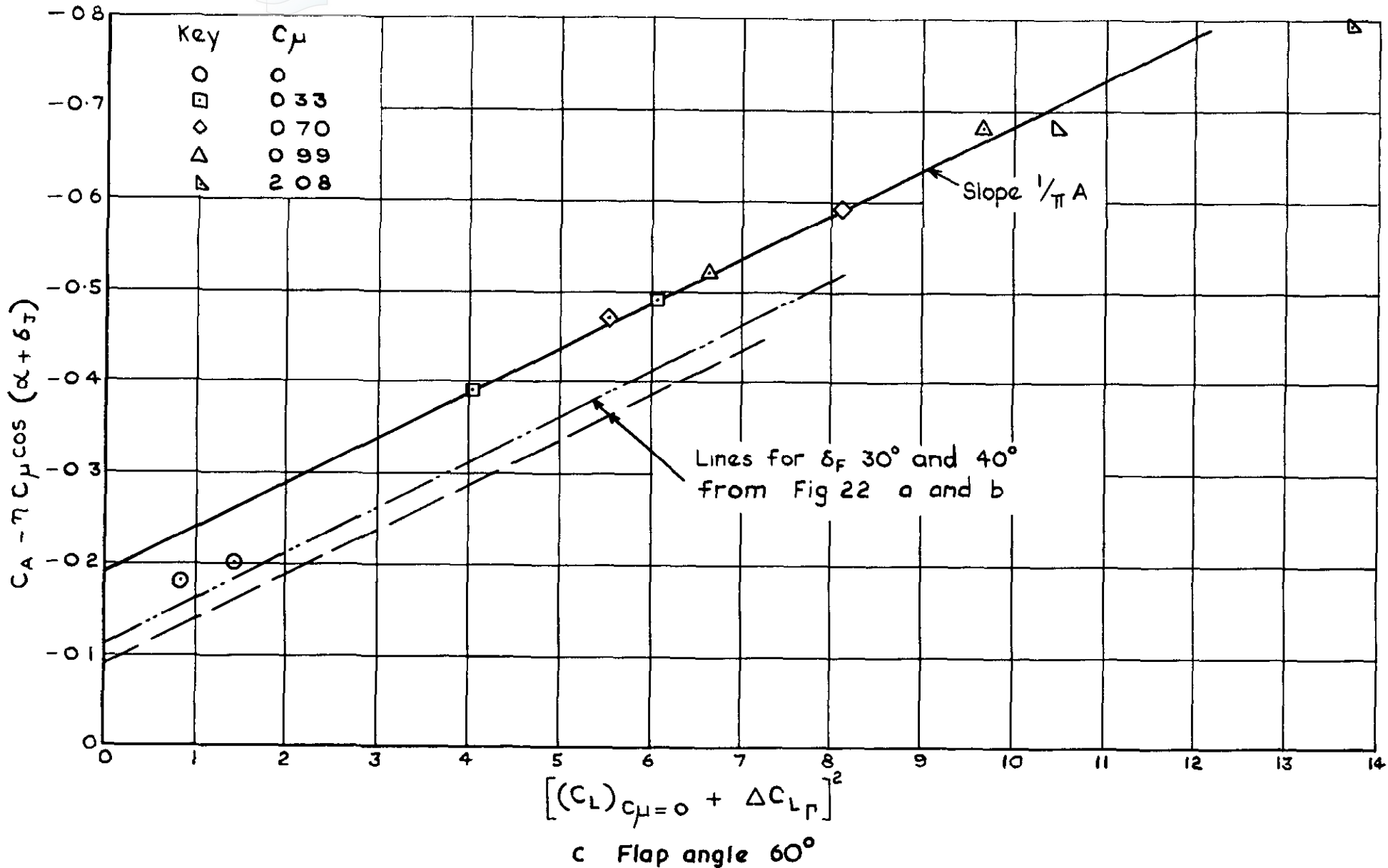


Fig. 22 cont Analysis of longitudinal force data from NASA TN D943 (Ref 10)



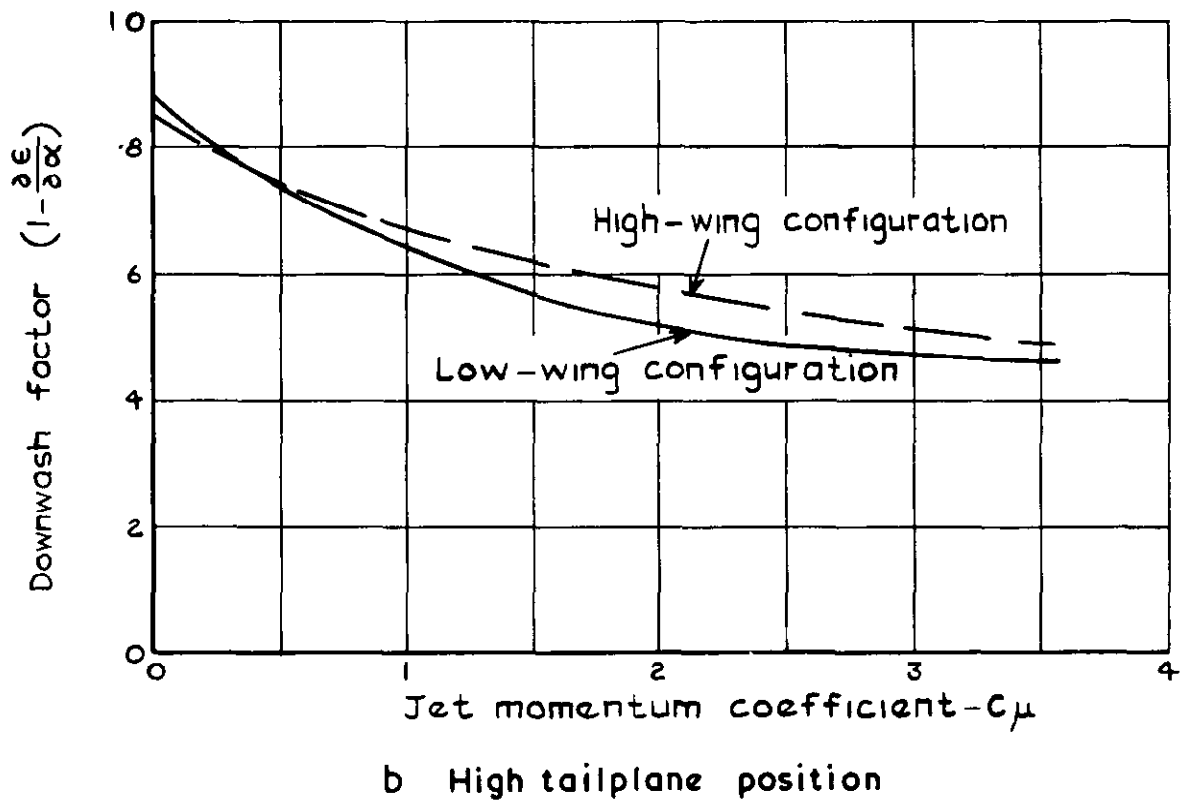
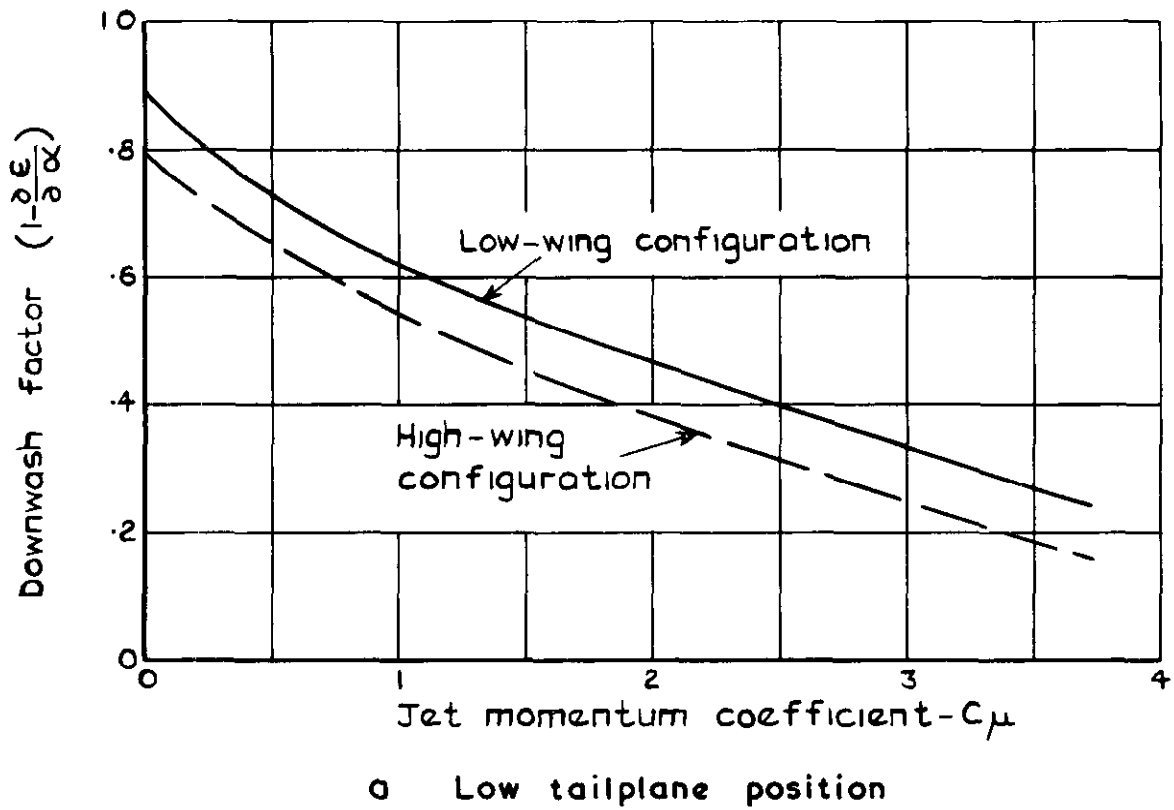


Fig 23a & b Variation of downwash factor with momentum coefficient for various configurations, from Ref 4



**DETACHABLE ABSTRACT CARD**

A.R.C. C.P. No 1194  
December 1970

533.694.6  
533.6 071

Perry, D H  
(with an Appendix by D. N. Foster)

**A REVIEW OF SOME PUBLISHED DATA ON THE EXTERNAL-FLOW  
JET-AUGMENTED FLAP**

The data given in thirteen NASA papers describing wind-tunnel tests on external-flow jet-augmented flaps are reviewed. Details are given of the configurations tested and the main results achieved. Some of the data is compared with theoretical work done in the UK in support of internally ducted jet-flap schemes.

The application of jet-flap theory to the correlation of maximum lift coefficients, based on considerations of leading-edge loading, is given in an Appendix.

A.R.C. C.P. No. 1194  
December 1970

533.694.6  
533.6.071

Perry, D. H.  
(with an Appendix by D. N. Foster)

**A REVIEW OF SOME PUBLISHED DATA ON THE EXTERNAL-FLOW  
JET-AUGMENTED FLAP**

The data given in thirteen NASA papers describing wind-tunnel tests on external-flow jet-augmented flaps are reviewed. Details are given of the configurations tested and the main results achieved. Some of the data is compared with theoretical work done in the UK in support of internally ducted jet-flap schemes.

The application of jet-flap theory to the correlation of maximum lift coefficients, based on considerations of leading-edge loading, is given in an Appendix.

The data given in thirteen NASA papers describing wind-tunnel tests on external-flow jet-augmented flaps are reviewed. Details are given of the configurations tested and the main results achieved. Some of the data is compared with theoretical work done in the UK in support of internally ducted jet-flap schemes.

A REVIEW OF SOME PUBLISHED DATA ON THE EXTERNAL-FLOW  
JET-AUGMENTED FLAP  
(with an Appendix by D. N. Foster)  
Perry, D H  
A R C C P No 1194  
December 1970  
533 694 6  
533 6 071





**C.P. No. 1194**

© *Crown copyright 1972*

Published by  
**HER MAJESTY'S STATIONERY OFFICE**

To be purchased from  
49 High Holborn, London WC1 V 6HB  
13a Castle Street, Edinburgh EH2 3AR  
109 St Mary Street, Cardiff CF1 1JW  
Brazennose Street, Manchester M60 8AS  
50 Fairfax Street, Bristol BS1 3DE  
258 Broad Street, Birmingham B1 2HE  
7 Linenhall Street, Belfast BT2 8AY  
or through booksellers

**C.P. No. 1194**

**SBN 11 470462 7**